CIRP Annals - Manufacturing Technology 00 (2024) 1–27

Contents lists available at ScienceDirect

CIRP Annals - Manufacturing Technology

journal homepage: https://www.editorialmanager.com/CIRP/default.aspx

Surface conditioning in cutting and abrasive processes

Volker Schulze (2)[a,*], Jan Aurich (1)[b], I.S. Jawahir (1)[c], Bernhard Karpuschewski (1)[d], Jiwang Yan (2)[e]

[a] wbk Institute of Production Science, Karlsruhe Institute of Technology (KIT), Kaiserstraße 12, 76131 Karlsruhe, Germany
[b] Institute for Manufacturing Engineering and Production Management, RPTU Kaiserslautern, Gottlieb-Daimler Strasse, 67663 Kaiserslautern, Germany
[c] Institute for Sustainable Manufacturing (ISM) and Department of Mechanical and Aerospace Engineering, University of Kentucky, Lexington, KY 40506, USA
[d] University of Bremen, Faculty of Production Engineering, Leibniz Institute for Materials Engineering IWT, Badgasteiner Str. 3, 28359 Bremen, Germany
[e] Department of Mechanical Engineering, School of Science and Technology, Keio University, Yokohama 223-8522, Japan

ARTICLE INFO

Article history:
Available online xxx

Keywords:
Cutting
Sensor monitoring
Control
Surface integrity

ABSTRACT

Cutting and abrasive processes affect the surface layer state of the components treated. This determines their performance in service. An adjustment of the surface layer properties would allow for enhanced performance. This paper introduces the influences of named processes on the surface layer state and their systematics. Models and sensor concepts for surface conditioning are described and combined to soft sensors which are the basis for active control within the processes. A validation study and actual applications of the conditioning concept are shown, allowing for further technological and scientific understanding of surface conditioning and its contribution to material and energy efficiency.

1. Introduction

All manufacturing processes influence the surface layer state of a component, which in turn significantly determines the properties of parts in service. Although it is intended to successfully exploit these effects, knowledge of the conditioning of the surfaces in the context of the final cutting and abrasive process of the component is still only very limited today. For surface conditioning in cutting and abrasive processes, mainly of metallic materials, not only geometric features but also the characteristics of the surface layer are determined and controlled as target values at the same time. This represents a paradigm shift in manufacturing, because process control variables that were previously fixed can now be varied within permissible limits in order to meet both objectives concurrently. The generation of the surface layer must be robust against disturbance variables in the process.

The surface conditioning concepts emerging in the horizon are compiled and presented in this paper. After presenting the relevant terminology in Section 2, Section 3 shows the major surface layer properties which may be induced in machining processes and their effects on the functional properties, which are mainly restricted to fatigue, tribology, and corrosion resistance. This section concludes with a compilation of measurement techniques for surface layer states which are evaluated according to their availability for in-process applications. Section 4 presents the established and upcoming models in the description of surface layers which were mainly physics-based and are increasingly shifting to data-driven as well as hybrid models. Their combination into soft sensors is the focus of Section 5 and is followed by the actual concepts available in active control of surface layer properties in Section 6. Finally, some first applications are described in Section 7, followed by a summary of the work presented with the outlook in Section 8.

2. Terminology: from surface integrity to surface conditioning

The functional performance of a component in operation is strongly influenced by the transformation of the workpiece in a machining process and can be assessed by functional properties. As part of the component properties, functional properties result from the component's geometry as well as characteristics of the bulk material and the manufacturing-related modified surface layer and can be determined in functional tests. The fact that, in addition to geometry, material characteristics, in particular of the modified surface layer, influence functional properties, was prominently addressed for the first time by Field and Kahles with the term "surface integrity", coined in 1964 [70]. They defined surface integrity as the inherent or enhanced condition of a surface produced in a machining or other surface generating operation" and released an extensive list of alterable surface layer properties (cf. Section 3) [71].

Subsequently, researchers and users have increasingly paid attention to the surface layer properties when designing components in order to achieve an improvement in surface functionality. In manufacturing technology, the deliberate generation of desired surface layer properties by a machining process—also known as the inverse problem of manufacturing because it

* Corresponding author.
E-mail address: volker.schulze@kit.edu (V. Schulze).

https://doi.org/10.1016/j.cirp.2024.05.004

determines the process parameters based on the resulting surface properties—has been an objective under the term “surface engineering”. With specified system parameters, the machining parameters considered as actuating variables that can be set at the respective machining device to control the machining process were investigated in terms of their effect on the surface layer properties. By means of correlations between machining parameters and resulting surface layer properties, effects have been established in the past. However, their validity is usually limited to the specific machining process and the range of the investigated system and machining parameters. In an international round robin test, conducted by a CIRP Collaborative Working Group on Surface Integrity and Functional Performance of Components between 2008 and 2010, it was impressively demonstrated how challenging the deliberate generation of specific surface layer properties on this basis remains. Most of the participating research institutes were unable to generate a surface residual stress of 200 MPa by a machining process of their own choice [121]. Accordingly, at that point in time it was not possible, or only possible to a very limited extent, to apply the existing knowledge in such a way that surface layer properties could be deliberately generated without an iterative approximation.

Among others, Brinksmeier et al. [33] pointed out that a detailed examination of the events during machining along the so-called chain of effects, also referred to as causal sequence in other contexts, (see Fig. 1)and the respective correlations within is necessary to solve the inverse problem in manufacturing without expensive iterations. In a first step, the process loads resulting from the machining process and its parameters are considered, which characterize the external impact on the workpiece. Here, a distinction can be made between mechanical, thermal, and chemical (main) impact or a combination of these, e.g., a thermo-mechanical impact, which is mostly the case for cutting and abrasive processes. Correlations between process loads and resulting surface layer properties already lead to a broader process understanding, but a transfer to another system and machining parameters remains challenging.

In a next step in the chain of effects, the internal material loads resulting from the process loads and energy conversion processes are considered. The material reacts to these on the basis of its specific material behavior by generating certain material modifications, which indicate changes in surface layer properties. In 2011 Brinksmeier et al. introduced the term “Process Signature” for all correlations between internal material loads and material modifications [30]. Accordingly, a knowledge-based predictive adjustment of a machining process in order to generate specific surface layer properties is achieved by utilizing the Process Signature and the further correlations within the chain of effects.

Establishing Process Signatures significantly depends on the ability to determine spatially and temporally resolved internal material loads (e.g., temperature- and stress-fields) and spatially resolved material modifications (e.g., changes in hardness and residual stresses) [32,34]. Especially the access to the internal material loading state during the process is not straightforward and has therefore to be complemented by models (cf. Section 4).

As the internal material loads reflect what the material experiences during machining, this allows a more general description of machining processes. However, until now it has always been assumed that the optimized machining parameters stay static. Even when Process Signatures are considered, surface engineering remains with the assumption that no disturbance variables occur that did not already exist when the correlations were established. In order to take into account these observable or hidden disturbance variables when solving the inverse problem in manufacturing, a closed-loop machining approach is available with surface conditioning (cf. Section 6) [248]. In contrast to surface engineering, this is a knowledge-based, in-process-management of surface layer properties. Thus, it requires a reliable surface layer state monitoring and a dynamic control of the machining process. Because conventional measurement technology is not able to measure surface layer properties during machining, soft sensors have to be developed that combine appropriate sensors with accurate and quick models (cf. Section 5). Fig 2 shows the chain of effects from the system and machining parameters to the functional properties and summarizes the described development from surface integrity to surface conditioning. Additionally, definitions of the terms explained in this section are given based on the work of a CIRP task force on a common understanding of the term “surface integrity” led by Brinksmeier and Meyer in 2018 and on the comprehensive glossary provided by Schulze et al. [228].

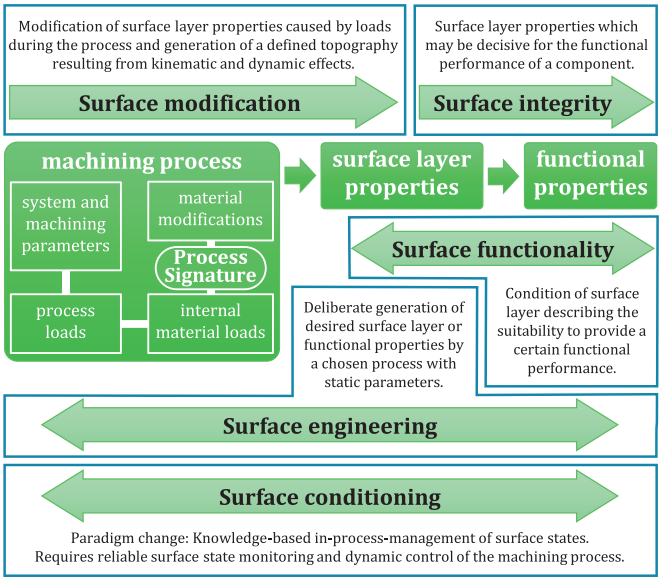

Fig. 1. Chain of effects and terminology from surface integrity to surface conditioning.

geometrical	mechanical	microstructural
		
• topography • roughness • cracks • ...	• strength • hardness • residual stresses • ...	• phase • inclusions • grain size • ...
optical	**magnetical**	**electrical**
		
• refraction • reflection • transparency • ...	• remanence • coercitivity • alignment • ...	• conductivity • permittivity • thermoelectrical • ...
	**thermal**	**chemical**
	• heat affected zone • conductivity • resistance • ...	• composition • alloys • oxidation • ...
		

Fig. 2. Surface layer properties.

3. Surface layer properties after cutting and abrasive processes

Surface layer properties can be subdivided into geometrical properties and material characteristics of the modified surface layer. Fig. 2 shows exemplary surface layer properties and a classification conducted by the CIRP task force in 2018. Since Field and Kahles's research, we know that the hardness, the presence of cracks, the microstructure, and the roughness of a machined surface as well as other surface layer properties can have a significant influence on the functional properties of highly stressed metallic components. These properties were part of a so-called "Minimum Data Set" of the American National Standard on Surface Integrity published in 1986 [242]. It was recommended to extend the set by parameters of residual stress distribution and behavior under cyclic loading in order to provide a "Surface Integrity Standard Data Set". The reliable determination of the residual stress state as well as the fatigue strength is associated with high effort, which severely limits the number of available results. The standard itself specifies more than 20 surface layer properties that can affect the functional performance and thus influence the surface integrity.

3.1. Correlation of surface layer properties with functional properties

In order to describe the functional performance of components, functional tests are carried out from which functional properties can be derived. Depending on the application, components must fulfill a wide variety of functional properties, e.g., optical, electrical, biological, magnetic, and esthetic properties. In this section, functional properties are restricted to mechanical, tribological, and chemical functional properties, as these are often the most important ones for machined components. Nonetheless, the concept of surface conditioning is applicable for all functional properties of interest. Within the three categories considered in the following, known correlations of these functional properties with correspondingly subdivided surface layer properties are described. Often, there is a pronounced interaction of several surface layer properties in these correlations. The evaluation of a separated influence of a single surface layer property is therefore difficult to achieve, but it is also not mandatory due to the likewise complex interaction during surface modification in machining.

3.1.1. Mechanical properties

Mechanical functional properties quantify the component's ability to withstand an applied load without failure or plastic deformation. The types of loading can be transverse, axial, or torsional. Besides static strength measures, cyclic loading reduces strength, thus fatigue strength is often more important for the in-service functional performance. Bending, torsion, and also notches lead to maximum stresses on the component's surface resulting in crack initiation and a lowered fatigue strength. This underlines the importance of surface layer properties after machining. For the characterization of the fatigue strength, cyclic stress is plotted against the cycles to failure in S-N curves and a distinction is made between low cycle fatigue and high cycle fatigue up to a fatigue limit, where an infinite number of loading cycles can be applied. Regarding fatigue strength, the component's topography can be of particular importance. Novovic et al. stated a non-negligible effect when the average surface roughness exceeds Ra $>$ 0.1 μm [188]. In another work, Novovic et al. investigated the high cycle fatigue of machined titanium alloy workpieces and separated the influence of the topography and residual stresses by means of stress relief annealing [187]. Again, it was proven that a low surface roughness results in a longer lifetime of the component. Moreover, compressive residual stresses also lead to a higher fatigue strength.

This was also found in the early work of Field and Koster, who demonstrated a direct influence of surface residual stresses after grinding on the fatigue strength of bending fatigue specimens [72]. It was shown that the fatigue strength could be more than doubled by the introduction of compressive residual stresses alone. Scholtes and Macherauch show results on the influence of milling on the bending fatigue strength [223]. In soft-annealed specimens of AISI 1045, tensile residual stresses of +210 MPa or compressive residual stresses of −300 MPa could be generated with otherwise similar surface layer properties. Despite differences in the magnitudes of the surface residual stresses of more than 500 MPa, the same S-N curves occur in both cases. Thus, the residual stresses have no influence on the fatigue strength. In contrast, hardened specimens of AISI 1045, in which surface residual stresses of different magnitude and sign were generated by different grinding parameters, show a strong influence of residual stresses on the fatigue strength. Compressive residual stresses increase the fatigue strength, while larger tensile residual stresses drastically decrease it. The fatigue strength therefore strongly depends on the material condition and the different stability of the residual stresses. Measurements after certain numbers of load cycles show that residual stresses are almost completely relieved until fracture in the normalized state, while they remain almost unchanged in the hardened state.

Smith et al. investigated the high cycle tension fatigue strength after hard turning of AISI 52100 steel [245]. The results revealed that the effect of residual stresses is more significant than the effect of a white layer and the fatigue strength is directly proportional to both the surface compressive residual stress and the maximum compressive residual stress.

Sasahara investigated the effect of surface residual stress and hardness resulting from different turning conditions (variation of tool nose radius, feed rate, and kind of tool edge) of AISI 1045 steel on rotating bending fatigue life (Fig. 3) [214]. Results show a higher fatigue life if compressive residual stresses and high hardness can be induced by the cutting process. This situation can be realized by applying a low feed rate, a small corner radius and a chamfered cutting edge tool. For hardened components, the calculation of the influence of the local combinations of hardness and residual stress depth profiles as well as roughness on the fatigue strength is possible using the concept of local fatigue strength or the weakest-link concept [25]. The local failure probability after multi-axial and irregular loading can be determined on the basis of statistically distributed irregularities in the component. Further conceptual approaches regarding the correlation between surface layer properties and fatigue strength are summarized in [159,226]. While the weakest-link concept focuses on crack initiation, crack growth-oriented approaches are presented in [159] showing the possibility of preventing cracks from growing due to residual stresses. A combination of evaluation of crack initiation and the ability of crack growth is developed in [227]. More sophisticated concepts are given by damage parameters introduced in [69,243].

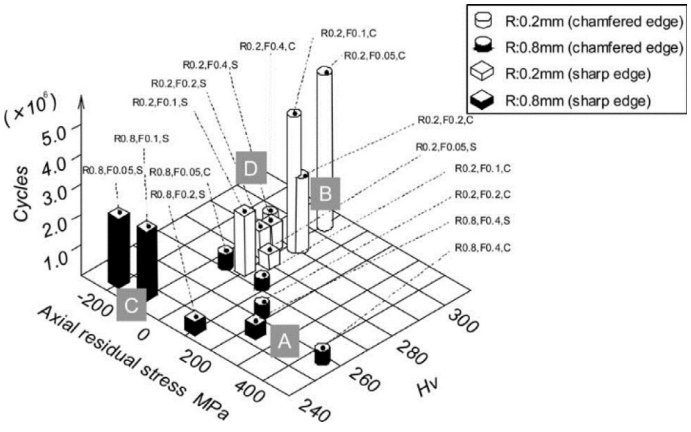

Fig. 3. Interaction of axial residual stress and hardness on fatigue life, grouped in four regions (A, B, C, D) [214].

3.1.2. Tribological properties

Tribological functional properties quantify the frictional and wear behavior by investigating the component after various contact tests. With regard to the friction and wear behavior of sliding and rolling elements, both the initial condition of the surface or the subsurface layer (e.g., topography, grain size, residual stresses) set by the manufacturing process and their dynamic changes during tribological loading are of great importance. The interrelationships have been investigated in the past in a fundamental oriented manner, e.g., on non-lubricated Cu pairs [14,117,206], but especially with regard to the running-in behavior of technical, lubricated sliding systems [23,49,217,218]. Within the tribological contact zone, depending on the initial grain size as well as the stress and environmental conditions, grain refinement can occur as a result of plastic deformation as well as grain coarsening due to grain boundary movement and dynamic recrystallization. At the same time, phase transformations, mechanical and chemical intermixing can be observed. This leads to the formation of a so-called third body, which under favorable conditions reaches a state of equilibrium of new formation and degradation through wear, which subsequently determines the friction and wear behavior of the tribological system [84]. The complex relationships and mutual interactions between friction coefficient, surface stress, and grain size mean that the relevant processes have so far usually only been described qualitatively.

Regarding the rolling contact fatigue of a hard turned specimen of AISI 52100 steel (62 HRC), Schwach and Guo isolated the effects of residual stresses by polishing to a roughness of $Ra = 0.1$ µm [229]. Their results confirm the importance of surface and near-surface residual stresses. They also reveal that a component without a white layer can have a lifespan six times longer than a component with a white layer. As the white layer increases in thickness, the fatigue life decreases.

For the same material, Guo and Waikar conducted sliding contact tests on a ball-on-disk tribometer at dry and lubricated conditions and different load levels [99]. A white layer generated in turning decreases the coefficient of friction, while grinding significantly increases the coefficient for dry conditions. For lubricated conditions, these results reverse.

Cho et al. analyzed the white layer by nanoindentation and revealed a higher elastic modulus, yield strength, and hardness than the bulk material [51]. In terms of wear resistance, the increased surface hardness can be beneficial. However, their results show a dependency on the load level. For high contact pressures, fast crack propagation can lead to delamination and reduces the wear resistance.

3.1.3. Chemical properties

Important chemical functional properties mainly quantify the corrosion behavior of components. As roughness increases the effective surface, corrosion resistance is affected by the topography. Walter and Kannan confirmed an increase in corrosion current and pitting tendency with increasing surface roughness of a magnesium alloy in chloride-containing environment [283]. The same is shown by various researchers for stainless steels [109,215,236,310], where pitting and the corrosion rate increases, and for copper [150], and titanium alloys [40]. Moreover, Prevey and Cammett revealed that a higher hardness increases corrosion resistance of aluminum alloys in a salt fog environment [197].

3.2. Mechanisms of generation of surface layer properties

Modification of surface layer properties can have mechanical, thermal, or chemical causes and, in the case of machining, often also simultaneous combinations of these in a highly nonlinear manner. Karpuschewski et al. [131] show the related mechanisms in a triangle spanning these three causes, see Fig. 4. In this section, mechanisms are explained in detail for changes in the topography, microstructure and hardness as well as residual stresses.

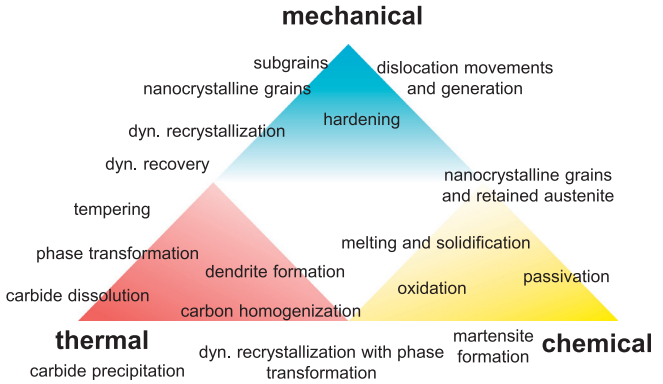

Fig. 4. Triangle of process loads and classification of induced mechanisms therein [131].

3.2.1. Generation of topography

Along with the purely geometric topography formation that takes place during machining due to a kinematic intrusion of the tool cutting edges with the workpiece, material mechanisms also modify the topography. In their comprehensive review, Liao et al. summarize these mechanisms [155]. As an important cause, they identify particles that are created during machining and get into the contact zone. These result in plucking, but also in surface tearing and grooves. In materials with a low ductility, cracks may originate from this. Further mechanisms are smearing due to the plastic deformation caused by the flank face and adhesion of material due to high contact stress.

3.2.2. Generation of microstructure and hardness

In machining, a combination of all three types of process loads are involved in modifying the microstructure and hardness. However, for the description of important mechanisms, their impact will first be discussed separately in the following section. The mechanical process load leads to squeezing of the surface layer and thus to shearing and high strains in the workpiece resulting in deformed grains and even grain refinement and sub-grains in a mechanically induced white layer. Dislocation lines slide through the crystal lattice until they accumulate at grain or phase boundaries and lead to the work hardening effect. Thus, the distortion of the crystal lattice significantly contributes to an increased hardness value in the measurement. For shot peening, Wohlfahrt developed a model described in [223,226] which separates effects of Hertzian pressure from the stretching of surface layers. Scholtes adopted this to cutting in [222]. This is shown schematically in Fig. 5.

The thermal process load rapidly heats the surface layer, followed by a rapid cooling due to self-quenching of the material and heat loss via metal working fluid. Due to the resulting temperature changes in time and space, the microstructure and hardness can be modified. Already comparatively low temperatures can lead to a softening/tempering effect and a reduction of hardness. When the recrystallization temperature is exceeded, dynamic recrystallization of highly deformed grains form a thermally-induced white layer. Even higher temperatures lead to solid-state phase transformation. For steels, a diffusive driven austenitization takes place and the unit cell structure changes from body-centered to face-centered cubic. Dependent on the following cooling rate, the grains transform into ferrite, perlite, bainite, or martensite. The martensitic transformation especially affects the surface layer by a strength-increasing grain refinement.

Please cite this article as: V. Schulze et al., Surface conditioning in cutting and abrasive processes, CIRP Annals - Manufacturing Technology (2024), https://doi.org/10.1016/j.cirp.2024.05.004

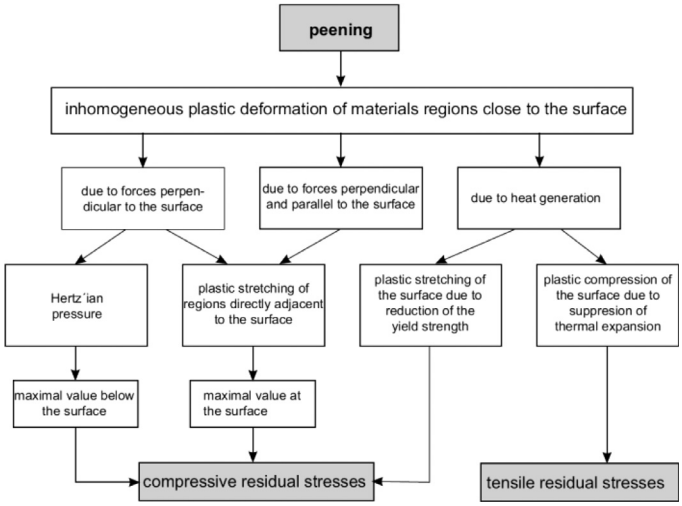

Fig. 5. Scheme for the evaluation of deformation processes during shot peening representing mechanical load [226].

3.2.3. Generation of residual stresses

A typical residual stress depth profile after machining shows compressive and tensile stresses in a "hook" shaped profile, where the thermal process load leads to tensile stresses in the near-surface layer and the mechanical load to compressive stresses with a greater influenced depth. During machining, the mechanical load initially causes compressive and then tensile stresses, which increase up to the yield point. The plastically strained layers are elongated and must be compressed by the residual stresses in order to maintain the cohesion of the solid. Thus, compressive residual stresses remain after unloading.

The thermal load also generates typical residual stresses. The surface layer expands with the temperature increase and leads to compressive stresses while machining. According to the temperature-dependent reduced yield point, the material deforms plastically. After cooling, the shortened surface layer must be lengthened by tensile residual stresses. This effect of thermal yielding can be outweighed by an opposite mechanism when materials with low transformation temperatures and a volume increase during transition from high to low temperatures are machined. As a result of rapid self-quenching, the solid-state phase transformation generates compressive residual stresses.

The thermal driven process is depicted in more detail in Fig. 6. Number 1 represents the compressive stresses in the surface layer, while this stress is partially reduced in number 2 following the yield strength. Without phase transformation, tensile residual stresses remain after cooling. In case of further heating, above austenitization temperature, compressive stresses are initially reduced in number 3 and, due to a higher thermal expansion coefficient, increased again. Number 4 represents the cooling, where the cooling rate plays an important role. For low cooling rates, tensile residual stresses again remain in the surface layer (number 5). High cooling rates lead to martensite formation and the accompanying volume increase generates compressive stresses in number 6, which remain in the surface (number 7).

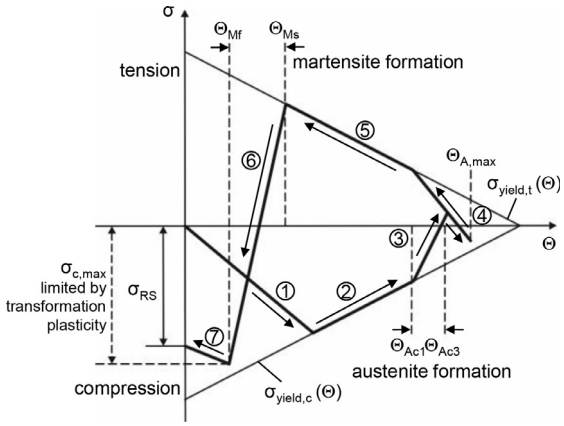

Fig. 6. Schematic illustration of residual stress formation in the surface layer during thermal loading [231].

3.3. Measurement of surface layer properties

The use of advanced surface characterization methods to assess the roughness and form errors of the machined surface, as well as the nature of the alterations produced in very thin layers of the machined surface is the key means to ensure that the machined parts meet application requirements, and in turn provides a reference for process optimization. The surface measurement can be classified in terms of conditions, as shown in Fig. 7 [80]. Among them, in-process measurement, which is defined as an on-machine measurement of workpiece surface carried out while the manufacturing process is taking place, is the ultimate form of measurement. Although extensive literature reviews have been carried out on surface integrity evaluation, the measurement conditions are non in-process [121,142,153,160,268]. Therefore, in this section we mainly focus on in-process measurement. Measurement technologies mentioned here include those that have already been used and those having potential for possible use in industry. These measurement approaches will also provide technical support for developing soft sensors which will be further discussed in Section 5. The measurement of surface layer properties will be discussed on the aspects of topography, microstructure, and residual stress, which is in line with the structure of Section 3.2.

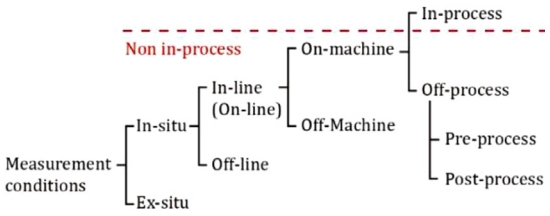

Fig. 7. Conditions of surface layer properties measurement (modified from Ref. [80]).

3.3.1. Measurement of topography

Optical measurement systems, such as white-light interferometer and confocal laser scanning microscope, and probe-scan systems, such as scanning probe microscope, are commonly used for characterizing surface form errors and surface texture. In the optical measurement systems, a light beam is projected onto a certain area of the workpiece surface for capturing the three-dimensional (3D) topographic information over an area. In the probe-scan systems, a mechanical or optical stylus attached to a displacement sensor scans the workpiece surface in a point-by-point or a continuous-path mode to trace the surface texture. Integrating the above measurement systems into machine tools by replacing the motion stage of the original measuring system with the machine tool axes, the workpiece surface can be measured on the machine tool that manufactured it, which is known as on-machine measurement systems. Gao et al. [80] provided a review of the surface metrology for precision manufacturing and discussed extensively on-machine measurement systems. Although these on-machine measurement systems can measure the workpiece topography with high accuracy, the machining must be stopped during the measurement to reduce the environmental problems that are

generated in the machining process, such as part vibration, and disturbances of chips and cutting fluids.

In the in-process measurement, to deal with the environmental problems, the use of sensors for indirect measuring is a possible solution. Angle-resolved scattered light (ARS) sensor is a state-of-the-art sensor for in-process measurement. Uebel et al. [264] developed a topography measurement system combining an ARS sensor and a pneumatic distance sensor, as illustrated in Fig. 8. The measuring point of workpiece surface is cleaned by dry ice from a pneumatic cleaning nozzle, and the pneumatic sensor is used to position the ARS sensor at the desired focal plane. A LED light source provides collimated light which is imaged onto the workpiece surface by a measurement objective lens. The workpiece surface reflects the light, and the reflected intensities are measured by the ARS sensor. This measurement process is very robust because the topography heights of the surface are not measured but rather their surface angles. As a result, high precision measurement data of the examined surface structures is obtained [232].

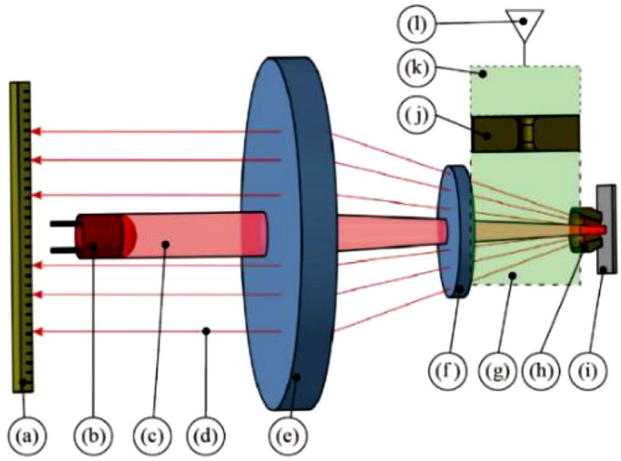

Fig. 8. Schematic layout of the opto-pneumatic ARS sensor: (a) linear PDA, (b) LED, (c) collimated beam, (d) scattering light, (e) lens, (f) window, (g) measuring chamber, (h) measuring nozzle, (i) workpiece, (j) pre-nozzle, (k) pre-chamber, (l) air supply (modified from Ref. [264]).

Also, monitoring machining characteristics is an effective method to in-process evaluate the variation trend of workpiece topography with less complexity and high suitability. For example, the use of acoustic emission sensors in the machining of brittle materials can characterize crack formations [90]. Sensors for measuring vibration, temperature, pressure, power consumption, and cutting force also have the potential to evaluate workpiece topography by observing the changes of the signals from these sensors [79,138], although these signals cannot quantitatively describe the topography.

3.3.2. Measurement of microstructure and hardness

Mechanical and thermal influence generated in machining processes can alter the microstructure of the layer near the machined surface. The conventional techniques for characterizing the microstructures of both metals and non-metals are X-ray diffraction (XRD), which detect surface oxidation/chemical reactions [89,140], phase transformations [304,306], and metallographic textures [167]; electron backscattered diffraction (EBSD), which measures lattice rotation [293], local dislocation/misorientation [115,177], and recrystallization/grain refinement [156,304]; and micro/nano indentation, which determines surface layer hardness [298,304]. Additionally, for non-metallic crystals, Raman spectroscopy and catho-doluminescence spectroscopy are widely used to detect phase transformation [296] and thickness of subsurface damage layer [7], respectively.

In-process measurements of the microstructure of steel/alloy surfaces have been well developed [37]. Micromagnetic Barkhausen Noise (MBN) is a typical proven technique for monitoring surface integrity [260]. An MBN sensor can detect the discrete jumps of magnetic domain walls in a varying magnetic field. The motion of these walls is influenced by mechanical properties such as residual stresses and microstructural features as grain sizes [220]. Therefore, MBN signals can be used to evaluate white layer formation [250] and phase transformation [181]. In general, if the surface and subsurface layers of a workpiece exhibit reduced hardness due to the thermal damage, the level of the MBN signal increases [106]. However, MBN sensors are not applicable when detecting nickel superalloys and titanium alloys due to the paramagnetism of those alloys. An Eddy current (EC) sensor is another suitable sensor, which can fill the gap left by the limitation of MBN sensors. When using an EC sensor, eddy currents are induced in the near surface of a workpiece by a primary alternating magnetic field generated by the test probe, as shown in Fig. 9. The magnitude of the eddy currents is influenced by workpiece microstructural features. At the same time, these eddy currents produce a magnetic field that opposes the field generated by the probe coil. The magnetic fields interaction is reflected in the voltage output. As a result, EC sensors are useful for white layer detection and macroscopic grain texture measurements [75,194]. Magnetic sensors exhibit high sensitivity to process disturbances such as vibrations, as they can result in variations in the sensor-workpiece distance or temperature fluctuations, leading to localized modifications in the magnetic properties [101]. Surface acoustic wave (SAW) sensors are also applicable to a surface microstructure detection because the propagation velocities of the surface acoustic wave (also known as Rayleigh waves) traveling along a workpiece surface are sensitive to the crystallographic texture. Using a laser to thermo-elastically generate a surface acoustic wave on a workpiece followed by capturing the frequency and wavelength of the generated acoustic wave, subsurface defects and crystallographic texture changes can be detected [36,244]. Additionally, acoustic emission (AE) sensors can capture the ultrasound bursts that emit from microcrack formations within the workpiece or the chip segmentation process [230].They are also used for monitoring the grinding burn phenomenon [130,157] and subsurface integrity [95,258] in the grinding of materials having low thermal conductivity. Similarly, cutting force sensors [173,247], temperature sensors [289], and thin-film sensors [85] have also been used to estimate white layer thickness and surface hardness during the machining process by analyzing the measured cutting forces and process temperatures.

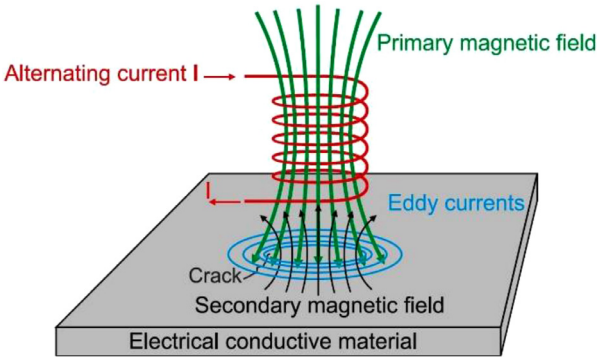

Fig. 9. Principle of eddy current testing [81].

3.3.3. Measurement of residual stress

The $\sin^2\Psi$ method-based XRD residual stress technique is the most common way to obtain residual stress in machined crystalline materials [93]. The stress is obtained from the slope of the relation of

the diffraction angle or lattice strain plotted against the $\sin^2\Psi$, where the diffraction angle is measured at several tilt angles Ψ of X-ray incidence by the zero- or one-dimensional sensor. Also, many attempts have been made to improve the measuring depth and analysis accuracy of residual stresses. For example, Genzel et al. [82] applied energy-dispersive diffraction for residual stress depth profiling in the zone deeper than 10 μm from the surface. Erbacher et al. [68] developed a method based on polynomials fitted to the "2θ vs. $\sin^2\Psi$ " plot obtained from XRD measurements to characterize residual stresses with steep gradients. By contrast, a new method called the "cosα method" using a two-dimensional sensor to obtain the crystal distortion is receiving extensive attention [253]. The stress analyzers based on this method are smaller in size and provide faster stress acquisition. Therefore, the cosα method is promising for the in-process measurement of residual stress. For non-metallic crystals, residual stress is also often measured using Raman microscopy. The value of the stress is determined by comparing the peak position in the machined area with that in the unmachined area [116,178]. For glass, optical tensor field tomography has been applied for automatic measurement of residual stress [2], which has potential as a sensor to use in the in-process measurement.

According to the working principle of Micromagnetic Barkhausen Noise and eddy current sensors mentioned in subSection 3.2.2, both sensors are capable of in-process measuring residual stress [3,124]. Junge [128] developed a predictive model of residual stress related to machining temperature and cutting forces, which consequently allows for evaluating residual stress by using temperature and cutting force sensors. Similarly, acoustic emission sensors can be applied to monitor tool wear conditions and then estimate the residual stress within the workpiece [230]. Moreover, combinations of sensors can be made to measure the surface integrity more comprehensively. Typical examples are micromagnetic multiparametric microstructure and stress (3MA) sensors, which combine Micromagnetic Barkhausen Noise, harmonic analysis of the tangential magnetic field strength, multi-frequency eddy current analysis, and incremental permeability for measuring microstructures and mechanical properties of ferromagnetic materials [28,291]. Table 1 summarizes the sensors that can be used in the in-process measurement of surface layer properties.

Table 1
List of typical sensors that can be used in the in-process measurement of surface layer properties.

Type of sensors	Determinable surface layer properties	Material limitations
Angle-resolved scattered light sensor	Surface roughness [264]	No limitations
Acoustic emission sensor	Surface cracks [90], surface burn [157,287], white layer [95,258], residual stress [230]	No limitations
Temperature sensor	Hardness and grain size [289], residual stress [128], surface burn [78]	No limitations
Cutting force sensor	Hardness [247], white layer [173,182], residual stress [128]	No limitations
Micromagnetic Barkhausen noise sensor	Hardness and residual stress [124], surface burn [143,180], phase transformation [181], white layer [35,219,251]	Ferromagnetic materials
Eddy current sensor	Phase transformation [75], residual stress [3], white layer [194]	Electrical conductors
Surface acoustic wave sensor	Subsurface defects [244], phase transformation [36]	No limitations
Micromagnetic multiparametric microstructure and stress analyzer (3MA) sensor	Hardness, microstructure features, and residual stress [291] , white layer [28]	Ferromagnetic materials

3.4. Correlation of surface layer properties with machining parameters

In this section, the influences of varying machining parameters on the resulting surface layer properties after cutting are presented. As already shown, the direct correlation between these two quantities is usually only valid for the specific use case. In the following, therefore, advanced approaches will also be presented which allow a material-oriented relationship by correlating the surface layer properties with process loads or internal material loads in Process Signatures. Furthermore, the section is subdivided into effects on the topography, microstructure, and hardness as well as residual stresses.

3.4.1. Effect on topography

During cutting, the shape of the tool is replicated in the workpiece surface, and roughness is mostly affected by the feed rate. For turning, for example, it is possible to determine the theoretical roughness $R_{z,th}$ or $R_{t,th}$ of a non-deforming material after machining on an ideally stiff machine tool by knowing the feed rate and the tool corner radius. Fig. 10 shows the dependence of two surface roughness quantities on the feed rate for hard turning of AISI 52100. The measured, as well as the theoretical roughness increase with increasing feed rate. However, especially at low feed rates, there is a deviation from the theoretical value, which increases quadratically with the feed rate and decreases linearly with the tool corner radius. The generated topography therefore also results from the interaction of mechanical and thermal loads. While the effects of machining parameters are not always unambiguous and depend on the tool and the heat treatment, clear trends can be identified. Regarding an increase of the feed rate, higher process forces must be taken into account.

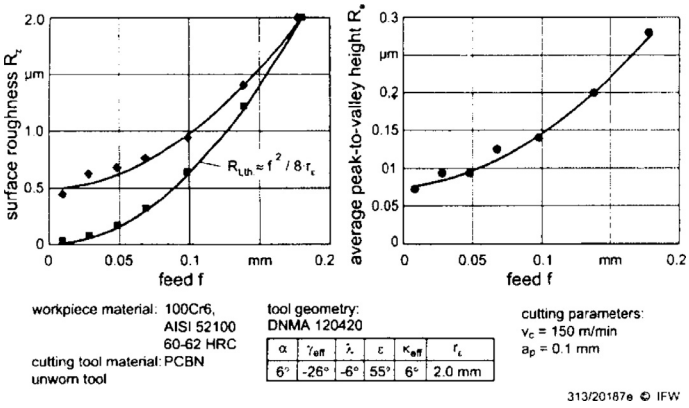

Fig. 10. Surface roughness after hard turning and its dependence on the feed rate [259].

The higher mechanical load results in greater tool deflection and an increased tendency for vibrations, as shown for example by Saini et al. [211] and Rech et al. [204]. An increase in roughness with increasing feed rate is thus also documented by many other authors, e.g., [257,268,302]. Increasing the cutting velocity initially leads to a reduction in the process forces, since the influence of thermal softening predominates over strain and strain rate hardening. As the cutting velocity is further increased, this behavior reverses and the process forces begin to increase. In high speed turning, cutting temperature and forces decrease again. In this context, the cutting forces are positively correlated with the surface roughness, i.e., a reduction can be observed [211,305], followed by an increase in the roughness [302]. An influence of the depth of cut on roughness has also been reported in literature, but the nature of it seems to depend on the specific process conditions. Thus, no influence as well as a positive and negative influence of an increased depth of cut on the roughness are found [211,257,268].

3.4.2. Effect on microstructure and hardness

Changes in microstructure and hardness are mainly studied for hard machining with geometrically defined and undefined cutting

edges. Bosheh and Mativenga analyzed white layers with a hardness above the bulk material when hard turning H13 steel [26]. With increasing cutting velocity, the width of the white layer and the hardness decrease. A reason considered is that more heat is carried away by the chips and less heat is transferred to the workpiece, in an even shorter contact time. This was also observed in a review by Yin et al. [302]. However, most of the works report an increase in white layer width when increasing the cutting velocity or increasing the feed rate [8,53,100,257,302]. These works reveal higher temperatures in the surface layer. Umbrello showed a hardness increase and a deeper layer of modified hardness when increasing the cutting velocity or the feed rate in turning of a Nickel-base superalloy [270]. Regarding greater depths of cut, Grzesik et al. [88] and Stampfer et al. [247] determined an increased hardness after turning of steels.

More advanced approaches can mainly be identified for grinding as temperatures are generally higher and modification in the microstructure is promoted. There are many works discussing the so-called "grinding burn limit", identifying a developing tempering zone and an unwanted softening of the microstructure of hardened workpieces. Pioneering work was undertaken by Malkin and Lenz [165] and Malkin and Guo [164] who defined a critical specific energy in dependence of the depth of cut and the tangential feed rate. Based on these findings, Heinzel et al. suggest that the critical limit can be better predicted by considering the contact time in addition to the specific grinding power [104] and developed so-called surface layer modification charts [103]. In Fig. 11 micrograph results for different grinding processes confirm the grinding burn limit and its dependence on the process load.

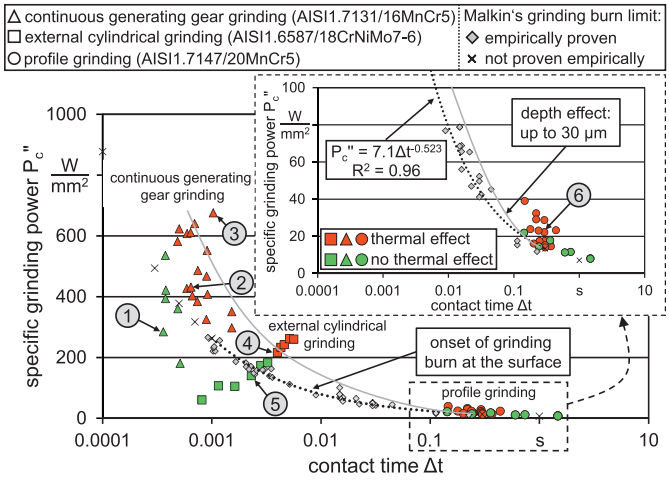

Fig. 11. Surface layer modification chart for different grinding processes [103].

Guba et al. even verified this critical limit for discontinuous profile grinding [91]. In addition, surface layer modification charts were developed, which represent the measured contact zone temperature over the contact time or alternatively over the tempering time [125]. Thus, for the occurrence of grinding burn, the validity of correlations could be demonstrated across materials and processes by means of process loads and internal material loads.

Kohls et al. were able to develop correlations for the material modification of hardness decrease with the Hollomon-Jaffe parameter as a characteristic internal material load for the combined effect of temperature and its change over time during grinding (see Fig. 12) [137]. For specimens where annealing effects with/without tempering zones and phase transformation were observed, individual Process Signature components could be derived.

Influences on hardness were also investigated in the adjustment of machining parameters for grind hardening. Heinzel et al. identified an area within the surface layer modification chart from Fig. 11

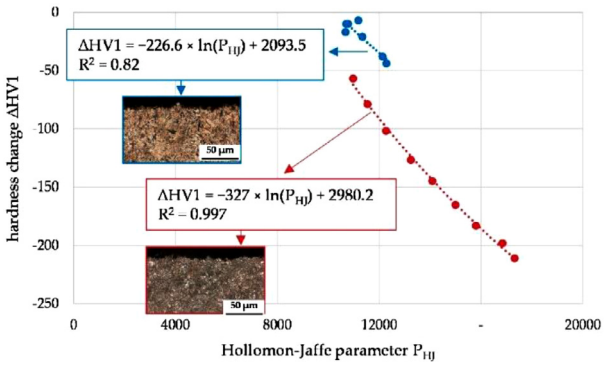

Fig. 12. Process Signature components describing the hardness change in grinding with no visible (blue) and visible (red) tempering zone [137].

where a hardness increase was achieved with different grinding processes [104]. Alonso et al. reveal a linear relationship between the specific grinding energy and the hardening depth after grind hardening of AISI 1045 [11].

3.4.3. Effect on residual stresses

The deliberate generation of beneficial residual stresses at the surface and depth profiles on the basis of varied machining parameters is the subject of a number of works. In general, it is stated that an increase in the feed rate leads to a shift of the surface residual stresses towards the tensile region due to higher thermal loads and to a shift of the subsurface maximum compressive stresses towards the compressive region due to higher mechanical loads [31,42,50,57,92,166,268,302]. An increase in the cutting velocity raises the frictional heat at the flank face and the dissipated heat in total. However, contact time decreases and more heat is carried away by the chips. Rech and Moisan [204] and Gunnberg et al. [92] determined a shift towards the tensile region at the surface for hard turning steel. The same was observed by Thakur and Gangopadhyay [257] and Chen et al. [50] after turning nickel-based superalloys. In contrast, Nowag et al. [189] and Brinksmeier et al. [31] identified a shift towards the compressive region after turning annealed AISI 52100. For the influence of increasing depth of cut, different indications can be found in the literature and no clear trends exists [257]. For hard turning, no significant changes in the residual stress depth profile are reported [42,57,92,166].

In a more advanced approach, measured residual stresses after orthogonal cutting of quenched and tempered AISI 4140 could be predicted by a Process Signature component from Buchkremer and Klocke [38]. Fig. 13 shows the dependence of specific areas for residual stresses on the stored mechanical energy and the experienced maximum thermal energy. The mechanical energy is the plastic work

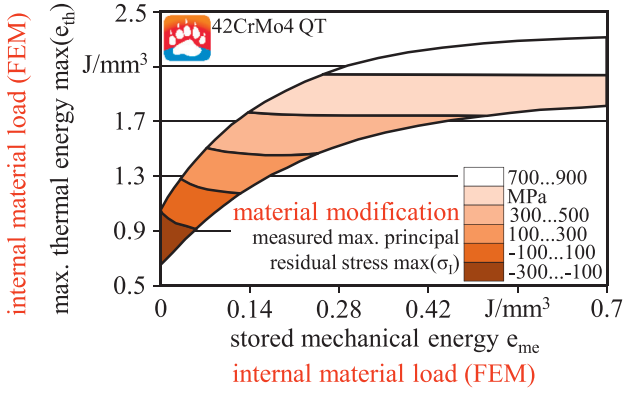

Fig. 13. Process Signature component describing the residual stress state in orthogonal cutting [34].

performed in a volume element of the workpiece material. The maximum thermal energy is proportional to the maximum temperature. Lei et al. adopted the approach by Buchkremer and Klocke for orthogonal cutting of AISI 304 austenitic stainless steel [146]. In the dependence of both energies, surface residual stresses and martensite content were evaluated.

In case of grinding, system and machining parameters offer a wide range of variations. Regarding residual stresses, Frerichs and Lübben adjusted these parameters in such a way that the mechanical impact can be neglected and modeling the process load by a moving surface heat source is acceptable [74]. Fig. 14 shows the resulting Process Signature components for the residual stress change at the surface. A characteristic internal material load has been found with the maximum temperature gradient. When temperatures are too low for austenitization, up to a gradient of approximately 100 K/mm, no residual stresses will be generated due to no yielding. Above this gradient, tensile residual stresses at the surface increase with increasing temperature gradient until an asymptotic behavior is reached. When temperatures are high enough for austenitization, a martensitic layer and compressive residual stresses at the surface are generated. The thickness of the martensitic layer decreases with increasing temperature gradient because the minimum temperature for initiating austenitization moves closer to the surface. At a maximum temperature gradient of 250 K/mm, maximum compressive residual stressed at the surface was achieved. For higher temperature gradients, the influence of this effect becomes smaller. Further Process Signature components have been developed regarding the depth of the zero crossings of the residual stress depth profile (see Fig. 15). The characteristic internal material load considers the maximum temperature and the square root of the contact time.

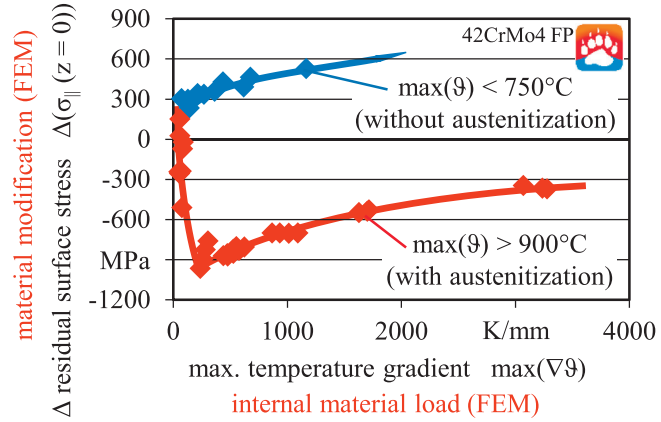

Fig. 14. Process Signature components describing the residual stress at the surface in grinding with a predominantly thermal impact [34].

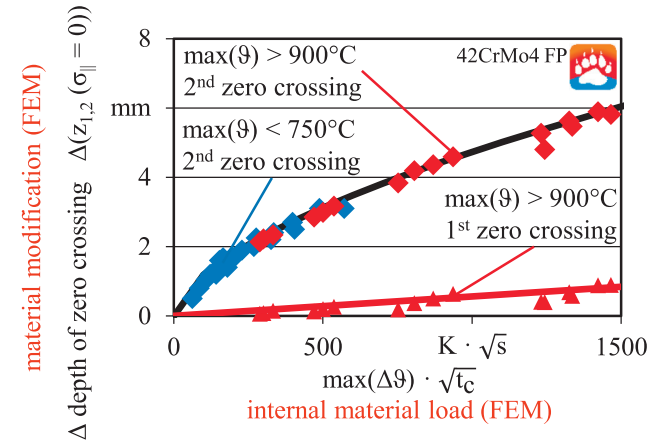

Fig. 15. Process Signature components describing the depths of zero crossings in grinding with a predominantly thermal impact [34].

In contrast to these results, Heinzel and Bleil adjusted the system and machining parameters in face grinding of annealed AISI 4140 in such a way that the mechanical impact becomes predominant [102]. This was obtained by increasing the specific grinding energy due to low cutting velocities, which results in a higher level of microploughing and more plastic deformation in the surface layer. The higher mechanical load can be seen in Fig. 16 with the increasing compressive residual stresses at the surface for increasing specific grinding energies.

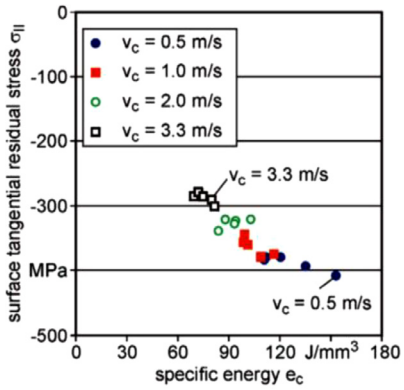

Fig. 16. Influence on residual stresses in grinding with a predominantly mechanical impact [102].

4. Modeling of surface layer generation in cutting and abrasive processes

4.1. Physics-based modeling of cutting processes

Pioneering early work on metal cutting in the late 1930s to mid-1940s by Dr. M.E. Merchant [172] was the beginning of physics-based model development. In 1995, the CIRP STC-C established a Cooperative Working Group on Modeling of Machining Operations, which resulted in two major activities with strong international collaboration: (1) an international workshop/conference series on modeling of machining operations starting in Atlanta, GA, USA [121] and lasting until today; and (2) a CIRP keynote paper on modeling of machining operations [279], which gave a first extensive review of all major models (analytical, numerical, empirical, and AI-based).

In 2007, CIRP STC-C established another new Cooperative Working Group on Surface Integrity, which produced a CIRP keynote paper [122] reporting modeling efforts in surface integrity by the research community. A subsequent CIRP STC-C collaborative work on modeling of machining processes resulted in another CIRP keynote paper [16], highlighting the need for physics-based analytical, numerical, and hybrid (i.e., analytical + numerical) models. A recent extensive review of the modeling of conventional machining processes by Melkote et al. [170] covers major milestones in the modeling of machining processes including analytical and numerical models developed for predicting machining performance and surface integrity. Outeiro et al. [192] conducted an extensive benchmark study to evaluate the numerical models for predicting machining performance and residual stresses on a range of materials (AISI 1045, AISI 316L, AISI 52100, Inconel 718 and Ti6Al4V alloy), with corresponding cutting tools (materials, coatings, and geometry). Major software platforms such as Deform, Abaqus, LS Dyna, and AdvantEdge were considered in the numerical simulations performed by different participating research laboratories. Simulated results were compared and experimentally validated. Very wide variations were observed in machining performance and residual stresses predicted by these software packages and these variations were attributed to varying boundary conditions and the constitutive relationships applied in the various models. Recent achievements on surface topography generation are summarized in the CIRP 2023 keynote paper [262].

Over the last two decades, numerous modeling efforts have been undertaken by the world research community for various materials. The major predictive modeling efforts on surface integrity are presented here below and are summarized in Table 2.

Table 2
Summary of major surface integrity modeling efforts in machining processes for three major material groups.

Material Group	Specific Material Modelled	Author(s)/ Reference (Year)	Modeling Methods	Predicted Surface Integrity Parameters
High strength hardened steels and difficult-to-cut materials	AISI 304 SS	Guo and Liu [98] (2002)	Thermo-elastic-viscoplastic explicit FEM, Sequential Cuts	Residual stress distribution
	Hardened steels (AISI 4340, AISI 52100) AISI 304 SS	Guo et al. [96] (2009)	Thermo-mechanical FEM Multi-scale modeling	Residual stresses, Hardened surface layer, Microstructure
	AISI 4340, AISI 316L SS	Liang and Su [152] (2007)	Thermo-mechanical analytical model	Residual stress
	AISI 316L SS	Valiorgue et al. [278] (2007)	Thermo-mechanical FE Model	Residual stress
	AISI 52100	Ramesh and Melkote [202] (2008)	Explicit dynamic FEM	Residual stress evolution, White layer formation
	AISI 52100	Umbrello and Filice [272] (2009); Umbrello and Jawahir [274] (2009); Umbrello et al. [275] (2010); and Umbrello et al. [276] (2010)	Thermo-mechanical FEM	White and dark layer thickness, Hardness, Microstructural evolution and Residual stresses
	AISI 4340	Agarwal and Joshi [6] (2013)	Physics-based analytical model	Residual stress
	AISI 52100	Ding and Shin [60] (2013)	Multi-physics model	Microstructure, Grain size
	AISI 4140	Tekkaya et al. [256] (2020); and Tekkaya et al. [255] (2023); Sadeghifar et al. [209] (2018)	Thermo-mechanical FEM and physics-based dislocation density model	White layer thickness, Grain size, Residual stress. Microstructural changes
Ni and Ti high-temperature alloys	Ti-6Al-4V, IN 718	Guo et al. [97] (2009)	Thermo-mechanical FEM, Multi-scale modeling	Residual stresses, surface layer, Microstructure
	Waspaloy (Ni-Cr based)	Lazoglu et al. [144] (2008)	Thermo-mechanical analytical model	Residual stress
	Ti and Ni alloys	Ulutan and Ozel [268] (2011); and Nieslony et al. [186] (2014)	Thermo-mechanical FEM	Microstructure, Surface layer, Residual stress
	IN 718	Wang et al. [285] (2017); Rinaldi et al. [207] (2019)	Numerical and empirical models	Residual stress, Microstructure
	Ti-6Al-4V	Caudill [45] (2019); Xu et al. [295] (2020); [294] (2021); Shi et al. [241] (2022); and Chen et al. [47] (2022)	Thermo-mechanical FEM	Microstructural changes, Grain size, Hardness
Lightweight Al and Mg alloys	AZ31B Mg alloy	Shen et al. [240] (2017); Pu et al. [200] (2014)	Physics-based constitutive FEM model	Hardness variation in the SPD layer, Microstructural changes, Grain size,
	AA7075-T65	Rotella et al. [208] (2013)	Physics-based constitutive FEM model	Hardness variation in the SPD layer, Microstructural changes, Grain size,

4.1.1. Models for the machining of high strength hardened steels and difficult-to-cut materials

Chen et al. [47] reviewed a large number of publications involving phenomenological models such as the Johnson-Cook (J-C) model, Khan–Huang–Liang (KHL) model, models considering strain-rate sensitivity (SRS), TANH model, modified Johnson-Cook model (JCM), etc.; physics-based models such as Zerilli and Armstrong model, Mecking and Kocks model, Viscoplastic self-consistent (VPSC) model, Johnson–Mehl–Avrami–Kolmogorov (JMAK) model, etc.; and models considering the microstructure evolution such as J-C model and JMAK-based dynamic recrystallization (DRX) model, TANH plastic model, models considering dislocation mechanisms, etc. They developed a novel constitutive material model for Ti6Al4V which integrates the well-known J-C model with a temperature dependent work hardening plastic model, while considering the influence of microstructural evolution and energy-density based damage evolution. Fig. 17 shows the predicted and experimentally obtained grain size distribution in machining of Ti6Al4V alloys for a range of cutting-edge radii and uncut chip thickness values.

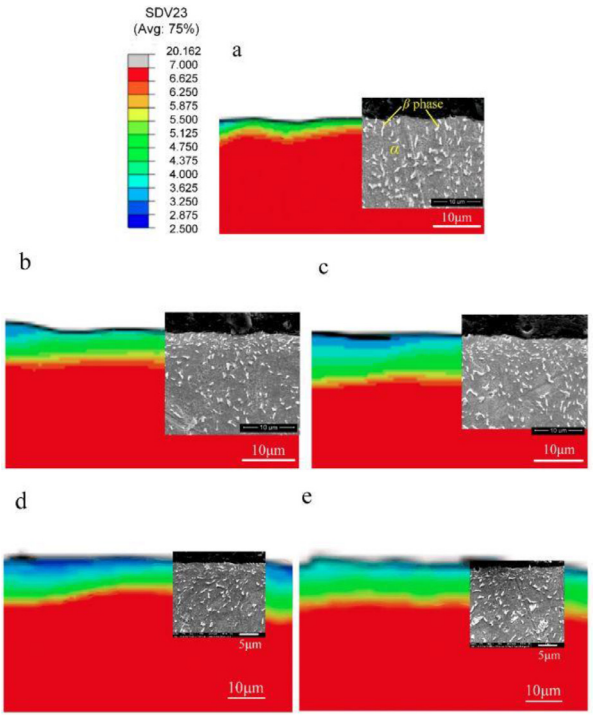

Fig. 17. Comparison of the predicted grain size distribution and machined sub-surface microstructure at different edge radii of (a) <5 μm, (b) 28 μm, and (c) 50 μm and at uncut chip thickness of (d) 30 μm and (e) 50 μm [47].

Abboud et al. [1] presented a numerical model for predicting surface residual stress in the machining of Ti-6Al-4V alloy for varying cutting conditions and cutting edge radius. Also, Chen et al. [47] recently studied machining-induced surface integrity and showed that in machining of an Ti6Al4V alloy under a range of cooling/lubricating regimes (Dry, MQL, LN2, Hybrid with LN2 and MQL) for varying cutting edge radii, the surface residual stress is heavily influenced by the cooling/lubricating strategy. Near-surface regions were shown to exhibit pronounced tensile residual stress states in dry and MQL machining (particularly the former). Hybrid cooling was shown to reduce the high surface temperatures generated during machining, thus mitigating the thermal mechanisms which drive the formation of tensile residual stresses, and allow for mechanical (i.e., ploughing) effects to dictate the resultant stress field. Thus, sustained compressive residual stresses were observed during hybrid machining.

With respect to Ni-based alloys, Ee et al. [66] presented a thermal elastic-viscoplastic finite element model to evaluate the residual stresses developed in machining with tools having varying edge radii and showed the effects of cutting conditions and sequential cuts with multi-passes. Variations of temperature and stress fields, along with the visco-plastic strain-rates, with time steps, were also shown.

For steels, Outeiro et al. [191] presented the effects of tool geometry, including cutting tool edge radius, tool coating, and cutting regime parameters on residual stress distribution in the machined surface and subsurface of AISI 316L stainless steel and developed a numerical model with elastic–viscoplastic FEM formulation, and validated their model experimentally. Their results also show that sequential cuts tend to increase superficial residual stresses. The thermo-mechanical analytical model presented by Liang and Su [152] for predicting residual stresses in machining considered the effect of cutting tool's hone radius (edge radius), and the model was validated in machining of AISI 316L stainless steel and AISI 4340 alloy steel. The analytical model presented by Agarwal and Joshi [6] for the prediction of residual stresses in orthogonal machining of AISI 4340 steel shows a good (86–88 %) agreement between the experimental and predicted residual stresses. It has been shown that on the machined surface, the tensile residual stresses decrease with increasing edge radius and increase with increasing cutting speed, and in the sub-surface, the compressive residual stresses increase with increasing depth of cut. More recent work by Tekkaya et al. [255] involves the prediction of white layer thickness and grain size in the machining of AISI 4140 steel and predicted the white layer thickness and grain size using Helmholtz free energy and Zener-Hollomon models which includes the effects of cutting edge radius on white layer thickness and grain size (Fig. 18). They also predicted the white layer thickness for varying tool rake angles, which shows no effect for tool rake angle variations from γ = +3, 0, −3, and −6°.

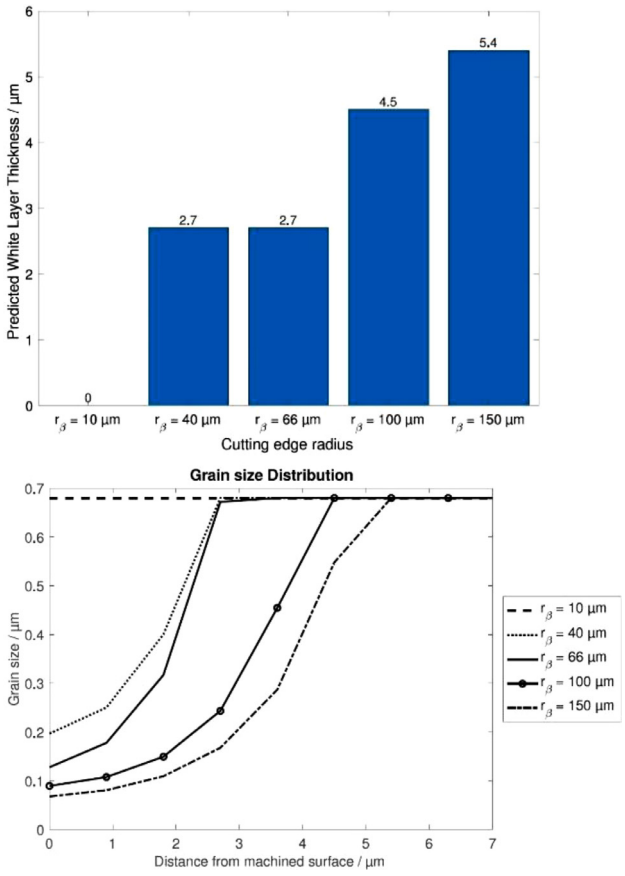

Fig. 18. Predicted white layer thickness and grain size in the machined sub-surface for varying cutting edge radii in hard machining of AISI 4140 steel [255].

Imad et al. [118], showed the effects of varying edge radii on surface integrity from using a 3D finite element model for the milling of hardened steels. Their numerical model was able to capture the effects of micro geometrical changes (between cutting tools of five different edge radii between 25 µm and 45 µm) on surface roughness, sub-surface plastic deformation, and sub-surface microhardness.

4.1.2. Models for machining of OFHC copper

Denguir et al. [58] presented a physics-based model for surface integrity prediction in the machining of OFHC copper. This model includes the plasticity, damage, and microstructural behaviors, and predicts the "classical" strain-rate and temperature effects and microstructural and the state of stress effects to improve the surface integrity prediction induced by machining.

Predicted values of residual stress, dislocation density, and grain size were also compared with experimental values showing that the proposed constitutive model gives better predictions when compared to the classical Johnson-Cook model [127]. Using a new physics-based "unified" material model Liu et al. [158] predicted the surface hardness for machining of OFHC copper, and this model seems to have captured the average grain size and dislocation density evolutions due to hardening, dynamic recovery, and dynamic recrystallization mechanism.

4.1.3. Models for machining magnesium alloys

Shen et al. [240] introduced a new physics-based constitutive model involving material plasticity and grain refinement utilizing both slip and twinning mechanisms and were implemented in a finite-element (FE) analysis for the multi-pass cryogenic machining of AZ31B Mg alloy. Microstructure evolution with nanocrystalline grain refinement was predicted, along with hardness variation and residual stresses in the sub-surface. The ultra-fine grain (UFG) layer produced with a larger, edge-radiused tool is far larger for both cases. Fig. 19 shows the experimentally determined grain size distributions in the UFG layers obtained from cryogenic machining AZ31B Mg alloy, with a grain size in the range of 30–60 nm. This is compared to those grain size distributions received from the numerical model of Pu et al. [200] incorporating the microstructural changes in the machining of the AZ31B magnesium alloy to study the effects of surface integrity under dry and cryogenic conditions.

4.1.4. Modeling of grinding processes

Much of the modeling research on grinding and other abrasive processes during the last two decades has focused on process modeling aiming at improved energy efficiency and economic benefits with high productivity. Very little work has been reported on the modeling of grinding processes for improved surface integrity or engineered surfaces and sub-surface defects generation. However, a significant number of researchers have attempted to model and predict surface roughness in grinding processes.

Early CIRP collaborative work by Tönshoff et al. [261] presented state-of-the-art knowledge on modeling and simulation of grinding processes and highlighted the need for the development of surface integrity models. Empirical topography models for surface generation including surface roughness predictions and surface residual stress were presented in this paper. Subsequent work by Hu and Chandra [113] presented a fracture mechanics approach for modeling the strength degradation in ceramics grinding processes. In this paper, the chip formation process was numerically modeled as a two-dimensional system of radial and lateral cracks to investigate the interactions of the radial and lateral cracks with various distributions of planar microcracks. Warnecke and Zitt [288] presented a new concept for process modeling with a software tool for analyzing and designing high

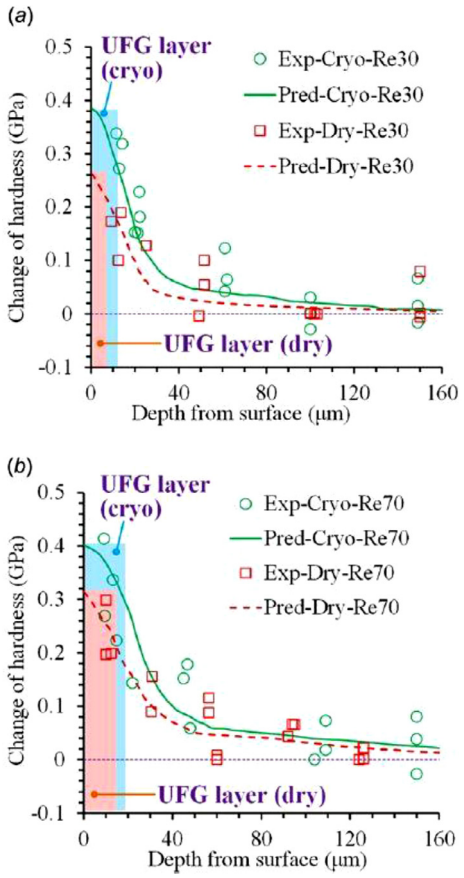

Fig. 19. Predicted microhardness profiles compared with the experimental measurements (Pu et al., 2012 [199], Experimental; and Shen et al., 2017 [240]—predicted).

performance grinding processes using kinematic simulation. Zhou and Xi [308] presented a new method for predicting surface roughness in grinding processes using the random distribution of the grain protrusion heights.

In a CIRP keynote paper, Brinksmeier et al. [29] reviewed the progress made in developing kinematic, analytical, and numerical models, along with molecular dynamic models for grinding processes, which provided a greater insight into the surface generation process in grinding. Comparison of measured and predicted surface roughness was also presented in this paper. This paper also shows the emerging rule-based models that were built on fuzzy logic for predictive model development in grinding processes. It presents a qualitative comparison of various models for grinding processes in terms of start-up requirements and the capability and effort requirements for modeling grinding processes.

Choi et al. [52] described generalized grinding process models for cylindrical grinding processes based on systematic analysis and experiments for predicting various grinding performance measures including surface roughness. Aurich et al. [18] introduced an analysis of different grinding models (analytical, numerical—FEM, BEM, and multi body simulation) by considering the machine tool kinematics and dynamics. Their simulation approaches are based on four different grinding processes (face grinding, speed stroke grinding, tool grinding, and NC-shape grinding) and are compared to experimental data in [107]. Agarwal and Rao [4] presented an analytical model for predicting surface roughness in grinding processes and compared the predictions with experiments. Subsequently, Li and Rong [151] modeled the grinding processes by considering grinding as a time-dependent process. They developed three-level models for: (a) grinding wheels to study the topographical and mechanical properties, (b) microscopic interactions to characterize the performance, and (c) process integration to understand the combined performance (Fig. 20). This model, among other parameters, was also shown to predict surface integrity and surface texture.

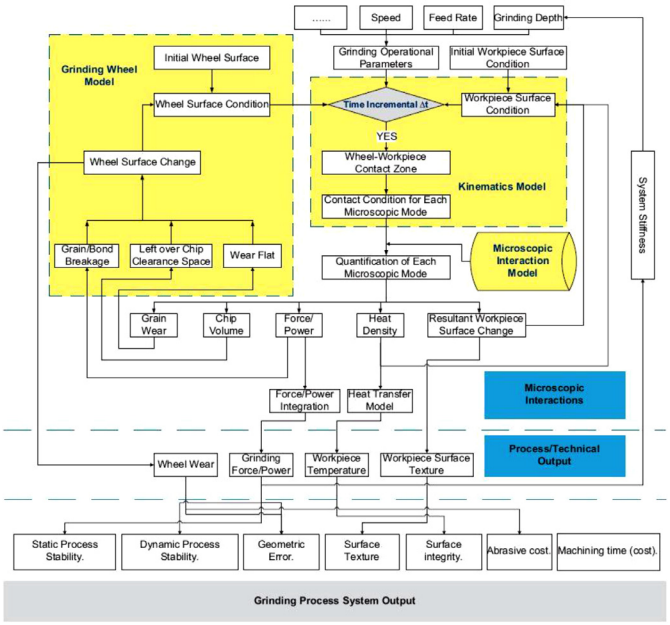

Fig. 20. The framework for a multi-level integrated predictive model for grinding [151].

Jiang et al. [126] developed a numerical model by considering the stochastic nature of the grinding process to predict the microscopic interactions. Predicted ground surface roughness values coincided well with the experimentally obtained values. Chen et al. [48] developed a new method to predict the gear surface profile generated by a grinding process by considering the random distribution of the grain protrusion heights, and compared the predicted and experimental surface roughness values. Aslan and Budak [17] developed a thermo-mechanical model to study the grinding process parameter effects on performance and compared the predicted and experimental surface roughness. Khare and Agarwal [134] also developed a simplified model to predict surface roughness in grinding and compared it with experiments. All these studies resulted in good agreements between model and experiment.

Zanger et al. [303] developed a discrete model for stream finishing and utilized it in surface modification analysis in AISI 4140 steel. They established a comprehensive correlation between process parameters, local contact conditions, and surface integrity. Fig. 21 shows the surface texture direction and comparison of surface texture before and after finishing. Setti et al. [234] conducted an analytical and experimental study of the surface generation mechanism in micro-grinding and studied the surface generation. They compared the surface texture and roughness on the ground surface for a range of operating conditions. Meng et al. [171] presented a critical review of predictive models developed during the last 15 years and presented the future directions.

4.2. Machine learning-based modeling

Due to the rapidly growing advances in the digitalization process (computation power, storage capacity, transmission rates), the amount of Machine Learning (ML)-based models which are utilized for the optimization of machining processes is increasing significantly [235,290]. Apart from tool condition monitoring and tool wear prediction [233], ML algorithms also offer great potential in

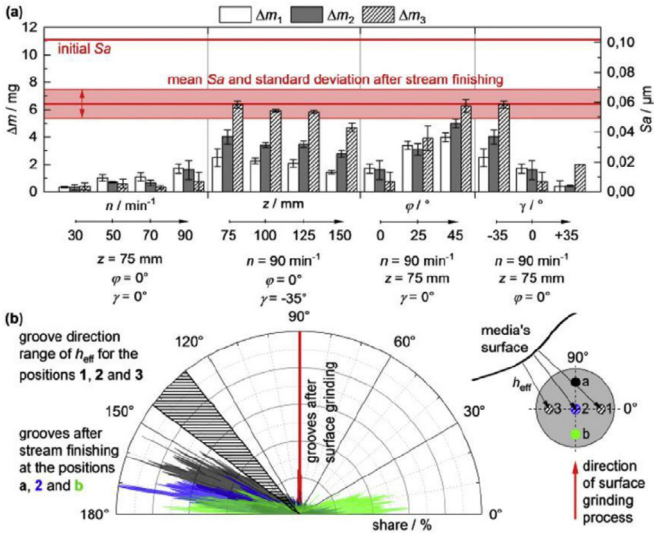

Fig. 21. Surface texture direction and comparison of surface texture parameter Sa before and after finishing [303].

modeling and predicting the surface integrity that is realized when machining [136,163]. Fundamentals of ML-based modeling as well as recent advantages and challenges for using these models to predict surface layer properties are presented in this section.

An ML model can be described as a function, assigning a suitable label or output to a subset of the input space. [129]. This predicting function is generally derived from an ML algorithm that is specified to learn the hidden relationships between the given input and output parameters. The application of ML algorithms consists mainly of the same phases which are data acquisition, modeling and its training, testing, as well as validation [201,267]. Since ML models are generally data-driven, the amount and especially the quality of the data provided highly impacts the performance of the model. Most input data is generated by measuring forces or power [195,224,292], acoustic emissions [174,216] and vibrations [62,162], which occur during the machining process. Despite having a severe impact on the machining process and the resulting surface integrity, the use of the temperature as an input parameter is only observed within a few investigations [83,87]. This can be explained due to the challenging experimental setup for temperature measurements, especially for cutting and abrasive operations. In this context, sensor fusion is a promising research field which aims to identify correlations between input and output signals using multi-view learning [10].

Aside from the data measured during machining, other process characteristics are also utilized as input data. Most prominently used are cutting parameters (cutting speed, feed, and depth of cut) [205,210,307] but also tool coatings [286], wear [280], or the workpiece material [73].

When the data has been acquired, data pre-processing, feature extraction, and feature selection are mandatory steps which highly impact the performance of the ML model [86,133].

Pre-processing typically includes but is not limited to [154]:

- Filtering and denoising
- Normalization and standardization
- Data labeling
- Data train-test-split

Feature extraction aims at a dimensional reduction of the input space while preserving all relevant information [133]. This generally results in a promoted accuracy, visualization, and comprehensibility [46]. For the feature extraction, statistical methods (e.g., standard deviation, power spectral density, skewness, crest factor, kurtosis) are utilized within the time and frequency domain [94]. The subsequent feature selection identifies the most relevant features using filter, wrapper, and embedded methods [41,179]. The ML model is trained with a defined and systematically structured subset of the collected data. The learning approach chosen generally depends on the problem that is to be solved (e.g., classification or regression).

A broad variety of ML algorithms are applicable to predict surface layer properties when machining e.g., Random forest [224,265], Regression analysis [185,210], and Decision trees [108,185]. However, when regarding literature, it is evident that the most prominently used algorithms applied are support vector machines (SVM) and artificial neural networks (ANN) [59,63,136,163].

SVM are linear models developed to solve either classification (SVC) or regressions (SVR) problems. These problems typically inhibit high-dimensional feature spaces which are solved by a regularized risk minimization approach using specific loss functions [39]. Here, kernel functions like the linear kernel, polynomial kernel, and gaussian kernel are frequently used to linearly separate the data with higher dimensional spaces [221]. ANN are directed graphs composed of nodes and their connections which are inspired by neural networks of biological organisms (see Fig. 22(b)) [130]. These nodes (neurons) are typically organized within layers and with labeling/activation functions [145]. Every ANN inhibits an input and output layer as well as various numbers of hidden layers in between. Nodes are the elementary functional units of the network as they receive weighted signals from the input layer or preceding neurons, processing them and forwarding them to subsequent neurons. The signal processing at the nodes is performed by (mostly non-linear) activation functions like the sigmoid function or the rectified linear unit (ReLU) function [225]. Due to the non-convexity and non-linearity of the activation functions used and the generally large networks, ANN are often harder to describe and explain in comparison to SVM. However, ANN often show favorable prediction performances if sufficient data is provided.

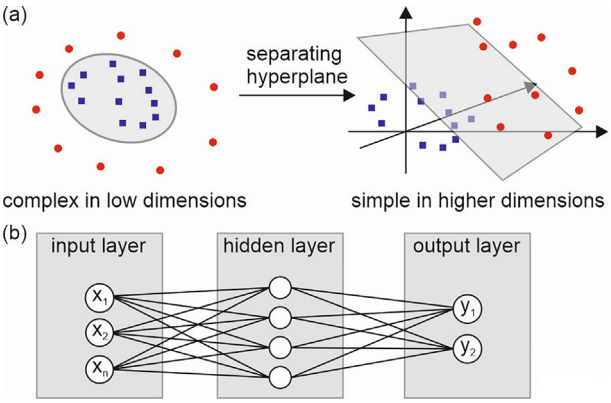

Fig. 22. Schematic depiction of the architecture regarding SVM (a) and ANN (b) [22,119].

The majority of ML models predicting surface layer properties focus on conventional cutting processes, especially milling [108,148,195] and turning [9,135,292]. Further applications are also found regarding grinding [210,216], drilling [224,286], and non-conventional machining processes e.g., electrical discharge machining [266] and abrasive water jetting [56].

The prediction and modeling of many surface layer properties has so far been conducted with very good results. However, most of this research focuses on the prediction of the surface roughness

[94,175,280,292,307]. This could be due to the fact that the surface topography is faster and less complex to characterize in comparison to mechanical and metallurgical properties within the surface layer. Regarding these properties, residual stresses are the most prominent feature being predicted [67,135,205]. Apart from that, there are also some studies focusing on the prediction of microhardness [252] or microstructure [83] within the surface layer.

Despite these recent advantages and the high potential of ML-based modeling, there are still obstacles to overcome to progress towards industrial applications. The main challenges of ML models refer to model overfitting and generalization issues [179,193].

Another main challenge with ML models is the size and quality of data, which must be acquired. As data acquisition is time consuming and generally results in high costs, DOE and especially the Taguchi method are often used to generate a suitable amount of data with a reasonable effort [61,297]. However, the quantity of the data collected is generally less important than its quality as irregularly sampled or noisy measurements are of little use and can lead to bias [141]. With this in mind, sensor failure is a challenging task, especially when using a single input source. Multi-sensor data acquisition can be a suitable solution, but is not a trivial task, since the collected data has to be synchronized, increases computational costs, and may result in potential redundancy of information [15,20].

In addition, generated ML models should be trained further, otherwise they might lose their prediction performance over time. This effect is known as concept drift which results from changes of the input data, the machining process, or the environment [12]. Here, transfer learning approaches offer the potential for a continual retraining or adaption of the model [149].

Another promising approach is the use of independent data sets in order to evaluate and improve the performance of ML models [237]. However, in order to use independent data, e.g., provided by published literature, availability and transparency of the whole ML modeling process is mandatory [86,163,237]. This is especially evident regarding data acquisition. While the measurement setup is generally described sufficiently, information about pre-processing and feature extraction are only provided by few authors. Despite that, the major effects of these steps on the performance of the ML model is widely accepted [86]. Consequently, it is highly recommended to provide sufficient information and data regarding all ML modeling steps within future literature to solve one major shortcoming of ML-based modelling [228,246].

4.3. Grey-box/hybrid modeling

The previous sections show that the use of physic-based and ML-based models for the prediction of the surface integrity after machining has been widely researched and can offer good results with sufficient accuracy. However, both model types are associated with intrinsic limitations that hinder a reliable application, especially for industrial applications. Physics-based models use *a priori* knowledge derived from rules and theories to formulate a model that aims to represent physical phenomena. Consequently these models may be founded on incomplete or inaccurate knowledge, or idealized assumptions, which decreases the accuracy of their respective predictions [300]. ML models are statistical models that use provided data sets to represent unknown systems. These statistical approximations are purely based on the features of the data values without incorporating the physical relationships within the system which is why no *a priori* knowledge is mandatory [238]. These models can compensate inaccuracies resulting from incomplete knowledge or simplified assumptions. However, their prediction accuracy is highly dependent on the generally large number of data sets that have to be provided [120,238].

Grey-box, or hybrid modeling stems from a modeling approach that aims at combining the benefits of domain knowledge (physics-based modeling) and empirical information (ML-based modeling) [139]. The term “grey-box” is derived from the mixture of white-box and black-box models. Here white-box models refer to analytical and physical descriptions while the black-box refers to the approximation of the unknown system via statistical analysis [139,300]. The grey-box modeling method is schematically depicted in Fig. 23. In general, these models inhibit a basic structure as they include general physical rules (white-box) while optimizing the parameters from actual experimental data sets (black-box).

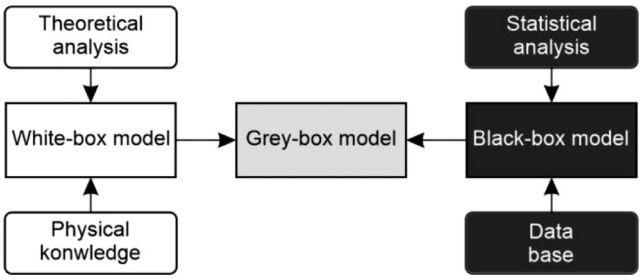

Fig. 23. Schematic depiction of the relationship between physics-based white-box, statistics-based black box, and hybrid grey box models [300].

According to Yang et al. [300], the development of a grey-box model is summarized by the following three steps:

- Construction of the system’s foundation using a knowledge- based model
- Identification of the system’s physical parameters based on the description of the system’s behavior
- Quantification of the identified parameters from experimental data

Grey-box models are generally divided into parallel and serial approaches [198]. The parallel approach utilizes both white-box and black-box models to achieve a sufficient prediction accuracy that would not be possible for an individual model e.g., due to incomplete knowledge of physical phenomena or a lack of suitable data sets [198]. Serial grey-box models are generally used to minimize uncertainties within a model. For example, the additional use of actual data can reduce uncertainties of an already established white-box model [64]. Additionally, results of multi-physics models can be used for the creation of training data sets as described in the CIRP 2023 keynote paper [262].

Although grey-box modeling offers a high potential to optimize prediction accuracy and therefore the machining performance, the amount of research dealing with the prediction of the surface integrity for machining operations currently remains very limited. This is especially evident when comparing with the research conducted using only white-box or black-box models. However, there is some research that uses grey-box models for milling [299], turning [271], and grinding operations [147].

For centerless grinding operations, Leonesio and Fagiano [147] developed a grey-box model to classify workpieces with suitable and unsuitable surface topographies. Due to the complex and often unstable process kinematics and the lack of available, suitable data sets, the application of white-box and black-box models produced poor results here. However, a hybrid approach combining a multi-class SVM with a physic-based, Low-Fidelity process model did result in a correct classification rate (CCR) of 97 %.

Yang et al. [299] used a serial grey-box model approach to predict residual stress profiles within the surface layer in dependence of the cutting parameters when peripheral milling Ti-6Al-4 V. First, a Johnson-Cook constitutive model is generated to predict the occurring loads within the surface-layer of the titanium alloy. The resulting residual stress profiles induced by the machining process

are then calculated using an exponentially damped cosine function. A statistical model was then established to optimize the fit between the simulation data and the residual stress profile using a particle swarm optimization method. Comparing the simulated profiles with measured residual stresses resulted in a prediction accuracy ranging from 81.7 % to 99.2 %. To describe these residual stress profiles, the surface residual stress, the maximum compressive stress and the penetration as well as the beneficial depth are identified (see Fig. 24). Via regression analysis, the model was further established to predict residual stress profiles in dependence of varying cutting parameters when milling. With an accuracy of 95.3 % to 97.8 %, the residual stress profiles were predicted in dependence of the cutting speed and the feed per tooth. As a result, the established model allows for optimum cutting conditions in order to control residual stress profiles for peripheral milling operations [299]. The prediction of residual stresses using a grey-box model has also been conducted for hard turning of AISI 52100 by Umbrello et al. [271]. The physics-based model is derived from a FEM that predicts the residual stresses in axial and tangential direction in dependence of the cutting parameters, the cutting edge geometry, and the material properties [273]. Based on the numerical simulation, an ANN was trained via backpropagation with a total of 86 data points (68 training, 18 testing) with varying cutting parameters (cutting speed, feed rate) and cutting edge preparations (chamfered, honed). After validation with experimental data sets, an accuracy of 84 % to 96 % was achieved [271]. By assigning the ANN a given residual stress profile, the grey-box model did also allow for a prediction of the process parameters that have to be supplied. For this inverse process design, the characteristics of the residual stress profiles (see Fig. 24) in axial and hoop direction were chosen as input parameters. Workpiece hardness, feed rate, cutting speed, and the cutting edge geometry of chamfered and/or honed cutting edges were set as output data. Validation via experimental data did result in accuracies between 86 % and 92 %. If the number of input data was reduced, the trained ANN model provided several options of parameter settings to achieve the desired residual stresses. When regarding several options it becomes possible to design the cutting process in a favorable way regarding other surface properties like surface roughness. For example, the solution with the lowest feed or highest cutting speed could be chosen in order to reduce surface roughness while still providing the residual stresses that have to be achieved. Thus the use of these type of grey-box models offer the potential to optimize total machining performance [271,300].

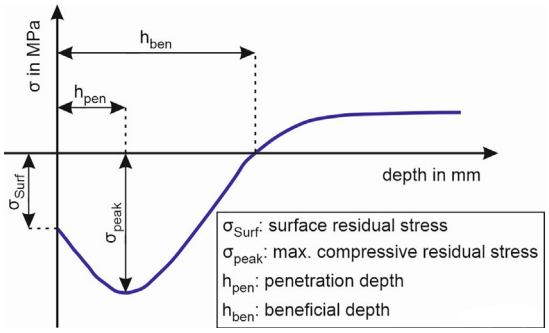

Fig. 24. Definition of a surface residual stress profile after machining [271,299].

5. Soft sensors for the estimation of surface layer properties

For surface conditioning in cutting and abrasive processes, not only geometric features but also the condition of the surface layer must be specified and controlled as target values at the same time. This requires real-time monitoring of surface layer characteristics by means of soft sensing technology and synchronous control of the relevant process parameters. In this section, we will focus on soft sensor technology, that is, the combination of representative sensor-measured variables and accompanying model/simulation to determine a target variable which is not measured directly but is calculated on the basis of correlating measured variables [228], as illustrated in Fig. 25, while the establishment of closed-loop control will be discussed in the Section 6.

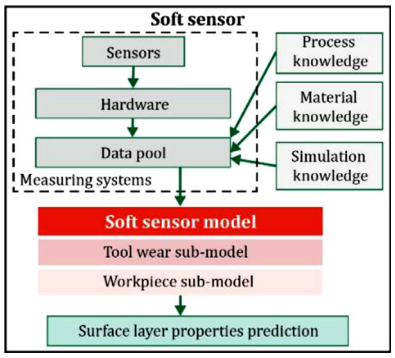

Fig. 25. General description of the soft sensor for surface layer properties prediction (modified from [28]).

As reviewed in Section 4, numerous researchers have developed various models, trying to correlate the manufacturing process with the surface layer properties. Therefore, it is important to couple these models with advanced sensors to construct soft sensors that can be integrated into the machining process. In general, there are two types of signals output by sensors. One type of signals presents the mechanical conditions during the machining, such as forces, temperatures, and the acoustic emission from tool-workpiece contact, which does not directly reflect layer properties changes in materials. The other type of signals presents material's conditions, such as the magnetic and electrical conductivity, as well as the acoustic emission from crack formation in materials, based on which the surface layer properties changes can be directly extracted and analyzed. Therefore, for the former type of signals, surface layer properties need to be assessed by the fusion of models with signals, which is discussed in Section 5.1. For the latter type of signals, since they are the result of the interaction of various material properties, the signals need to be carefully interpreted to separate a certain surface layer property, which is discussed in Section 5.2.

5.1. Fusion of models with sensor signals

Cutting forces are the most obvious signals that respond to mechanical machining. An example of a cutting, force-based soft sensor is schematically illustrated in Fig. 26, which is developed for the estimation of the maximum white layer thickness [173]. Machining parameters, including cutting speed v_c, uncut chip thickness h, and width of cut b, are used as a first input. Cutting force signals are collected in real time by force sensors and are imported into an analytical temperature model to compute the heat partition into the workpiece and the steady state temperature fields for the given specific cutting conditions. Subsequently, the maximum depth of white layer is predicted according to a dynamic recrystallization model in which the recrystallized grain size is determined by the temperature. In this soft sensor, the cutting forces are used for determining the temperature which affects the material microstructure changes. As an alternative, owing to the fact that hardness, residual stress, and white layer formation in workpiece material can be a function of tool flank wear [181,182,247,251], the force signal can also be used to predict in-process tool wear [54], consequently to estimate changes in surface properties.

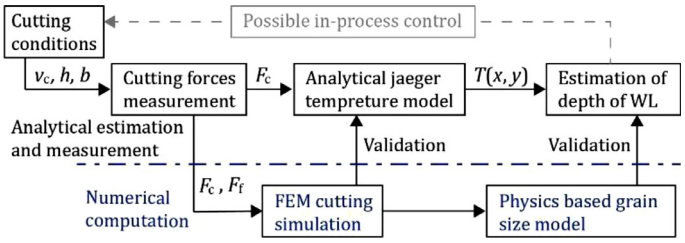

Fig. 26. Schematics of a cutting force-based soft sensor for the estimation of the maximum white layer thickness (modified from [173]).

Since machining temperature greatly influences the changes in surface layer properties, temperature is also an effective input signal for soft sensors [196,289]. Fukuhara et al. [78] embedded a thermocouple in a grinding wheel to monitor the changes of entry temperature, maximum temperature, down slope after the maximum temperature, and finish temperature in real time. The state of grinding wheel surface and the grinding burn phenomenon were identified after a series of empirical criteria. To better understand the interrelationship between the thermomechanical effects and the resulting residual stresses, Junge et al. [128] performed a combined measurement of the interface contact temperature with a tool-workpiece thermocouple and the components of the resultant force. They introduced a C-value, which has an approximately linear relationship with the axial residual stresses, as illustrated in Fig. 27. Therefore, substituting the in-process forces and temperature signals into the empirical formula presented in Fig. 27, compressive residual stresses in the axial direction can be obtained.

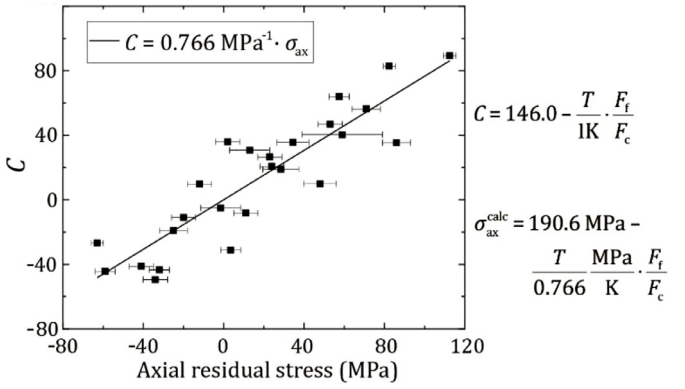

Fig. 27. Relationship between the C-value and the axial residual stresses σ_{ax}, as well as their linear fit for the calculation of the axial residual stresses σ_{ax}^{calc}. (modified from [128]).

In cutting processes, chip segmentation frequency correlates with tool wear, because the tool wear causes an increase in the tool-work material friction, which leads to an increase in the deformed chip thickness [184,230]. Several researchers have reported the relationship between acoustic emission signals and tool wear conditions [5,284]. Therefore, an acoustic, emission- based soft sensor can be realized by importing the tool wear calculated by AE signals to the function between surface layer properties and tool wear, the flow chart of which is similar to the cutting force-based soft sensor shown in Fig. 26. On the other hand, in grinding process, Tönshoff et al. [258] reported a correlation between the measured values of the parallel residual stresses near the surface and the root mean square value of the acoustic emission signal of a grinding experiment. This empirical model may be useful when developing soft sensors for grinding.

5.2. Interpretation as surface layer properties

Micromagnetic Barkhausen Noise (MBN) sensors have found potential applications in in-process measurement surface layer properties in ferromagnetic materials. The output signals M, which are the intensity of the discrete jumps of domain walls when Coercivity field strength H is applied, will be influenced by workpiece micro-hardness, residual stresses, and grain size. In general, MBN amplitude decreases if white layers are formed at the workpiece surfaces, because white layers have an elevated number of grain boundaries owing to their nanocrystalline structure and show high dislocation density, which impedes domain wall movement [250]. On the other hand, the MBN amplitude generally increases with increasing remanence, so that compressive residual stresses lead to a low MBN amplitude and tensile stresses lead to a signal increase [124]. The root mean square (RMS) value of the MBN is a potential indicator of austenite-martensite phase transformation, as it gradually increases with increasing volume fraction of martensite [183].

Strodick et al. [250] performed cutting experiments with various cutting parameters and measured maximum MBN amplitude M_{max} during the cutting process, as shown in Fig. 28 (a). After the cutting, cross-section specimens were made for observation of the white layer, as shown in Fig. 28(b), trying to correlate the detected M_{max} with the microstructure of the subsurface zones of the specimens. All specimens that had a white layer at the surface edge zone showed significantly lower M_{max} as well as a low standard deviation of MBN, whereas specimens without a white layer had higher M_{max} and a higher standard deviation between the values measured. Therefore, the M_{max} signal of MBN proves to be an adequate mean for in-process detection of white layers. However, since the white layers have a dominating effect on M_{max} signals of MBN, additional characteristics of the surface edge zones, e.g., residual stresses, cannot be identified by means of M_{max} signals of MBN.

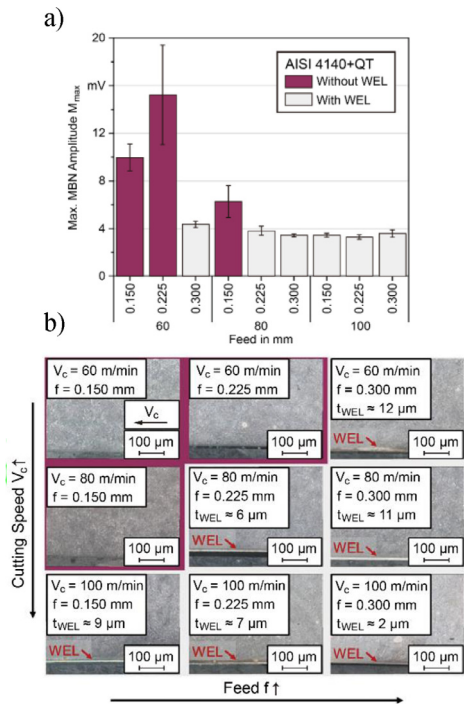

Fig. 28. Results of the (a) micromagnetic investigations, and (b) metallographic investigation in drilling of AISI 4140+QT [250].

Instead of using M_{max} signals of MBN as the only indicator, Jedamski et al. [124] recorded the time-resolved evolution of parameters M_{max} and M_{mean} (amplitude averaged over one magnetization cycle) in grinding steel, as shown in Fig. 29(a). With the start of material removal, both measured signals rise steeply and reach a plateau. Then, M_{max} remains unchanged at the same level until the end of spark out. In contrast, the value M_{mean} decreases from the beginning of spark out. Without grinding wheel contact,

Please cite this article as: V. Schulze et al., Surface conditioning in cutting and abrasive processes, CIRP Annals - Manufacturing Technology (2024), https://doi.org/10.1016/j.cirp.2024.05.004

the initial and final values of M_{mean} differ only slightly, while M_{max} remains at an elevated level. This suggests that the excitation of the MBN by the external magnetic field is further influenced by another effect during grinding, which has not been clearly understood thus far. Under three specific material removal rates, by comparing the in-process measured M_{max} and grinding forces (tangential force F_t, normal force F_n) (Fig. 29(b)), as well as measuring residual stress depth profiles and surface hardness after grinding (Fig. 29(c)), it is proved that M_{max} signals of MBN can be used to in-process detect changes in residual stress. However, further investigations on in-process quantitative residual stress determination are needed.

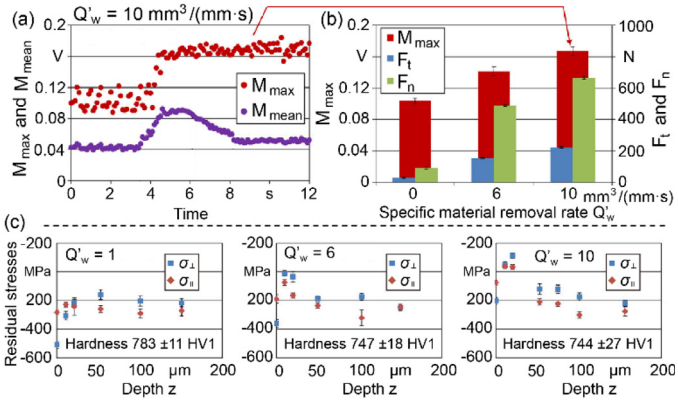

Fig. 29. (a) Typical M_{max} and M_{mean} signals during grinding process. (b) Average and standard deviations of M_{max}, tangential and normal forces. (c) Depth profiles of axial residual stresses and tangential residual stresses of the ground surfaces, (modified from [124]).

According to the principle of eddy current sensors introduced in Section 3.3 (see Fig. 9), the transformation of an austenitic microstructure with paramagnetic properties into a microstructure with ferromagnetic properties, such as martensite, is accompanied by a significant change in magnetic permeability and therefore shows a great influence on the eddy current signal. Pure austenite does not distort the waveform of the measurement signal with respect to the excitation signal. In contrast, the non-linear magnetic hysteresis in ferromagnetic materials produces higher harmonics in the measured signal.

Among them, the 3rd harmonic is particularly suited to provide information about the martensite volume content of the workpiece, as illustrated in Fig. 30 [75,76]. The formation of martensite is detected more accurate using eddy current sensors and modulating the excitation frequency than using the magnetic testing method [75]. The higher the excitation frequency, the lower the measurement depth. As a result, the distinction between the different martensite contents within the subsurface becomes clearer when using a higher frequency. In other words, when detecting lower martensite contents, a higher frequency is needed. Therefore, it is possible to determine the martensite content using the amplitude of the 3rd harmonic provided that a suitable excitation frequency is employed.

Since the characteristic dependence of the electric conductivity on stress, eddy current can also be exploited for residual stress profiling in certain materials. Botko et al. [27] examined the response of the eddy currents to the cutting-induced residual stresses in steel materials. They converted the measured values of horizontal shift of voltage and vertical shift of voltage measured with a EC sensor into the factors of phasor size and phasor angle, and then plotted the dependence of phasor size and phasor angle of eddy currents on residual stress, as shown in Fig. 31(a) and (b) respectively. The linear trend of the average value of EC phasor size with residual stress is statistically significant with a high correlation coefficient (R^2 = 0.9075), while the phasor angle has a

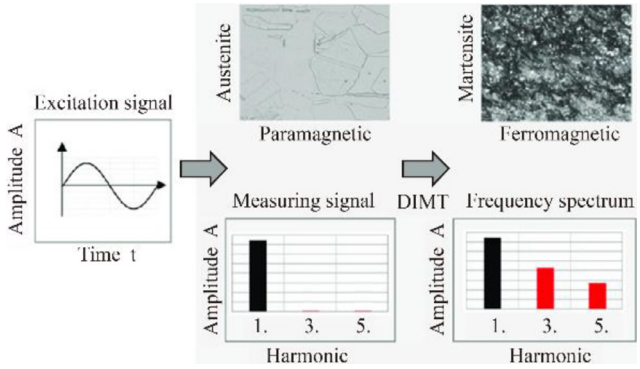

Fig. 30. Schematic illustrating eddy current testing with analysis of the higher harmonics that are caused by deformation-induced martensite transformation (modified from [76]).

lower correlation coefficient with residual stress (R^2 = 0.7002). Therefore, phasor size is an effective indicator for the in-process measurement of residual stresses when using an eddy current sensor. Acoustic emission sensors can not only be used to predict tool wear and thus estimate surface layer properties, but also directly monitor the changes in materials. The most common application is the monitoring of grinding burn, because when overheating a workpiece surface, a little transient source of acoustic emission due to thermal stress will be created [157,287,301]. However, since the AE produced by friction of tool-workpiece overlaps the signals generated by the burn, the use of appropriate signal processing techniques is crucial to accomplish the burn location. According to Távora et al. [254], the error of the location is less than 4 %.

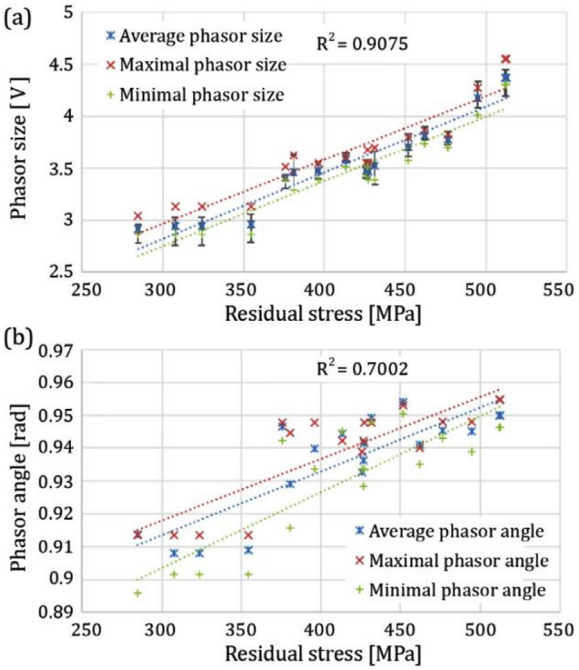

Fig. 31. Dependence of (a) phasor size and (b) phasor angle on induced residual stress. (modified from [27]).

6. Functional properties by control of processes

In contrast to conventional phenomenological approaches based on establishing correlations between the machine tool, process parameters including potential disturbances of these and the resulting geometry and surface layer state, the strategy of Controlled Functional Properties is based on the mechanism-based

hypothesis, that the fundamental thermal and mechanical loads imposed by the process will determine the surface layer state. This is combined with the available sensors plus models and the previously introduced soft sensors, which can be used in-process to receive real-time information on the actual state of the surface layer. The remaining challenge is to react in the process on deviations and therefore actively control the process in order to assure certain surface layer properties and therefore functional properties. This section will show the current state of the art with regard to strategies for active control with results based on a recently completed round robin activity focused on this topic.

6.1. Strategy of closed-loop control of surface layer properties

Fig. 32 shows the generic scheme of a surface-oriented process control system as a basis for the surface conditioning [228,248]. Set values are classically the geometry but here the surface layer state is also included. In the machine, the manufacturing process, its disturbances due to changes of the material state, wear of the tool, and other factors yield in variations of the set parameters. As they cannot be measured directly in-process, the soft sensor-concept is applied in order to close the control-loop with the observed values of the surface layer properties to be controlled. This provides the possibility to permanently determine the proper set values and therefore finally the functional properties of the part.

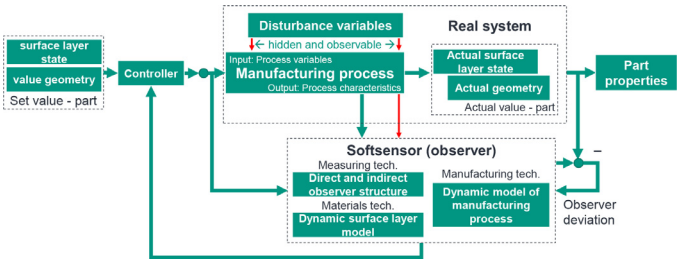

Fig. 32. Approach of closed-loop of the DFG priority program 2086 "surface conditioning in cutting processes".

Fig. 33 shows the generalized approach to access the machine control for a write–store–read of digital information, regardless of the type of control or measurement method. Starting from the process, a sensor or a measure from the programmable logic controller (PLC) of the machine allow for data acquisition (DAQ) in a digital manner, which is handled in the Field-Programmable-Gate-Array-Module (FPGA). Here, the measures are combined with the process model to the soft sensor and are applied to the controller. It generates an output to the override-input of the PLC or to an edge-PC, which is directed to the PLC of the machine, where the process itself is adapted. Edge also offers further cloud handling of process data. This allows for continuous measurement of the target surface properties with a reasonable cycle time [248] and further quasi-real-time adjustment at the machine within the process.

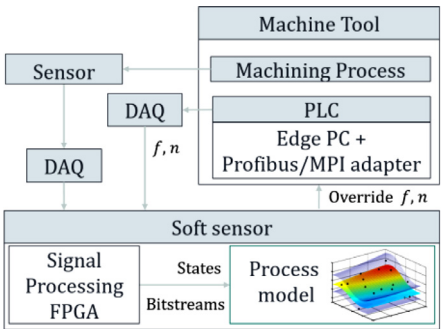

Fig. 33. Generalized approach to access the machine control.

6.2. Validation of the strategy

The control approaches presented require validation in a real industrial environment on machine tools. For this purpose, an international round robin test was set up in which the compensation concepts adopted by the different institutions involved were compared. The target variable was the residual stress profile in the surface layer characterized by a value of $\sigma_{ax,surf} < 200$ MPa at the surface and a value of σ_{ax} = -500 ± 100 MPa at a depth of 100 ± 25 µm during the external longitudinal turning of AISI4140 (42CrMo4) quenched and tempered at 450 °C for 1 h. The disturbance variable to be compensated was flank wear. For the tests in external longitudinal turning, coated tools of the company Walter AG of the type (ISO) CCMT120404-RP4 WPP20S with chip breakers were used. Detailed geometric features of the tools and their orientation are listed in Table 3.

Table 3
Specifications on the geometry of the tools provided for the participants.

Tool geometry	Value
Geometry	Rhombic 80°
Nose radius r	0.4 mm
Clearance angle α	7°
Macroscopic rake angle γ	0°
Principal cutting edge angle κ	95°
Cutting edge inclination λ	0°

In order to verify the initial processing, a reference cut using an unworn tool with cutting parameters indicated in Table 4 was specified. For compensating the influence of three predefined levels of flank wear on the resulting residual stresses, the feed rate f and the cutting speed v_c could be adjusted, while the depth of cut a_p should be kept constant. The final specimen geometry with three shaft sections for the compensating cuts and one for the reference cut is shown in Fig. 34.

Table 4
Parameters of the experiments.

Parameter	Value
Cutting speed (reference cut) v_c	200 m/min
Feed rate (reference cut) f	0.05 mm
Depth of cut a_p	0.2 mm
Width of the wear marks in the test points	< 0,1 mm 0.15 mm 0.25 mm

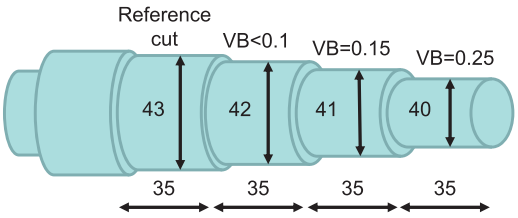

Fig. 34. Geometry of the specimens (dimensions in mm).

The X-ray analysis of the surface layer and the measurement of the residual stress values were carried out at the Bochum University of Applied Sciences, Bochum, Germany, using the cos-α-method. The measurement depths prepared by means of electrochemical machining and other measurement parameters can be found in Table 5.

In the series of experiments, a total of eight different concepts were investigated to compensate the influence of tool wear on the

Table 5
Parameters for the X-ray residual stress measurement.

Parameter	Value
Measurement depth	0, 25, 50, 100, 150, 200 µm
Device	pulstec µ-X360S
Radiation	Cr-K-Alpha
Method	Cos-alpha
Angle of incidence	35 ° {211}
Spot diameter	approx. 4 mm
X-ray Young's modulus	210,000 MPa
Poison ratio	0.3
Accuracy	+/- 30 MPa

residual stress profile. These can be divided into numerical and empirical models and are accomplished by the application of knowledge collected in literature. For the numerical methods, the process parameters were determined using 3D simulations of the process or substitute models. At the Leibniz Institute for Materials Engineering (IWT), Bremen Germany, the machining parameters were determined on the basis of a 3D-FEM chip formation simulation based on [281,282]. The calculated and measured residual stress profiles as a function of the feed rate were compared and validated based on the process forces. A similar approach was applied at the École Nationale d'Ingénieurs de Saint-Étienne (ENISE), Lyon, France. In their experiments, the process parameters were determined using the MISULAB FEM-software and validation using experimentally determined cutting forces [65]. In addition, the parameters were optimized using residual stress measurements. A different numerical approach was applied at the Institute of Production Science (wbk) of the Karlsruhe Institute of Technology, Karlsruhe, Germany. Here, 3D chip formation simulations were used to calculate thermomechanical loads, which then were applied to the workpiece in a substitute FEM-model of the turning process [65]. The concept, resulting in shorter calculation times, was verified by residual stress measurements [247,249].

Other experiment series were carried out based on empirical methods. Researchers at the Institute for Production Engineering and Photonic Technologies (IFT) of TU Wien, Vienna, Austria, chose an approach based on passive forces during machining. Constant passive forces were assumed to result in constant residual stresses. At the Institute for Manufacturing Technology and Production Systems (FBK) of TU Kaiserslautern, Kaiserslautern, Germany, results of turning experiments with varying cutting speed, feed rate, and tool wear within ranges derived from literature were correlated empirically with the resulting residual stresses measured using the borehole method (Stresstech PRISM system) [309]. In addition to the investigations at the research institutes, tests were also carried out in industrial companies. At the Timken Company, Canton, Ohio, USA, Barkhausen noise measurements were used to control residual stresses in order to compensate tool wear based on empirical findings. Other round robin participants did not carry out any empirical determination or simulation of the process parameters themselves, but used already-published results from the literature. During the series of experiments at the Laboratory for Precision Machining and Nano Processing (PMNP) of Keio University, Yokohama, Japan, trends known from literature were taken into consideration, such as the fact that compressive residual stress increases with cutting speed [161,239], that the flank wear increases the depth of the residual stress profile [55], or that decreasing the feed rate decreases residual stress [42]. Similarly, researchers at the Laboratory for Machine Tools and Production Engineering (WZL) of RWTH Aachen University, Aachen, Germany, also considered the literature. Here, counteracting effects of process parameters and tool wear on the residual stresses were taken into account. This can be summarized thus: in relations like compressive axial residual stresses decrease with increasing feed rate [42,43,114,176,203,212] and cutting speed does not significantly affect the axial residual stress profiles [190,203,213], that orthogonal cutting experiments show deeper compressive residual stresses with increasing cutting speed [44], and that worn tools produce lower residual stresses and lead to a greater depth of engagement [176]. Fig. 35 shows an overview of the process parameters as they were applied by the participants in the round robin. The blue arrows indicate whether this value was increased, decreased, or kept constant compared to the previous cut or the reference cut. The variation of the process parameters in the different approaches is indicated by arrows.

		Cut 1 *VB* < 0.1 mm		Cut 2 *VB* = 0.15 mm		Cut 3 *VB* = 0.25 mm	
Number	Method	Cutting velocity in m/min	Feed in mm	Cutting velocity in m/min	Feed in mm	Cutting velocity in m/min	Feed in mm
1	Numerical	150 ↓	0.2 ↑	150 →	0.25 ↑	200 ↑	0.25 →
2		200 →	0.05 →	200 →	0.05 →	200 →	0.1 ↑
3		100 ↓	0.1 ↑	200 ↑	0.15 ↑	300 ↑	0.2 ↑
4	Empirical	250 ↑	0.08 ↑	175 ↓	0.05 ↓	160 ↓	0.03 ↓
5		200 →	0.05 →	180 ↓	0.04 ↓	65 ↓	0.012 ↓
6		80 ↓	0.5 ↑	60 ↓	0.5 →	40 ↓	0.5 →
7	Literature	300 ↑	0.02 ↓	270 ↓	0.04 ↑	150 ↓	0.03 ↓
8		200 →	0.05 →	200 →	0.05 →	200 →	0.05 →

↓ → ↑ = Modification from the previous cut

Fig. 35. Process parameter adjustments applied in the round robin.

The results of the experiments performed on 8 specimens are given in Fig. 36 and Fig. 37 at the reference cut and the 3 cuts using the differently worn tools. It can be seen that the residual stresses at the surface are mainly in the tensile area and do not show a clear tendency with the wear state but range up to about 500 MPa, which is clearly out of the intended range. In contrast, the residual stresses at a depth of 100 µm are mostly in the compressive area but mainly in the range below 150 MPa with their absolute value. Only a few values are higher and only a single one approaches −400 MPa. With increasing wear, there is a tendency to obtain higher compressive residual stresses. Nevertheless, all residual stresses are far below the intended value. In total, it needs to be stated that all the different compensation strategies did not lead to the intended distributions of the residual stresses nor could they keep these constant with the wear state. This means that substantial developments are necessary in order to achieve a successful compensation of disturbances in technical cutting operations.

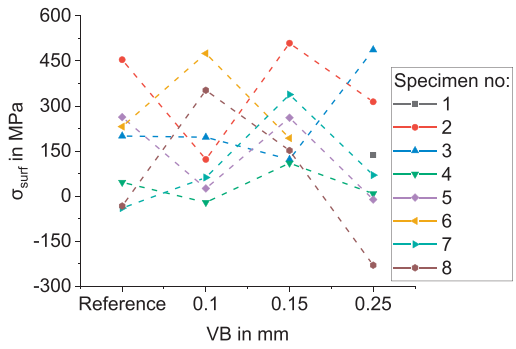

Fig. 36. Axial residual stresses at the surface in each segment of the specimen.

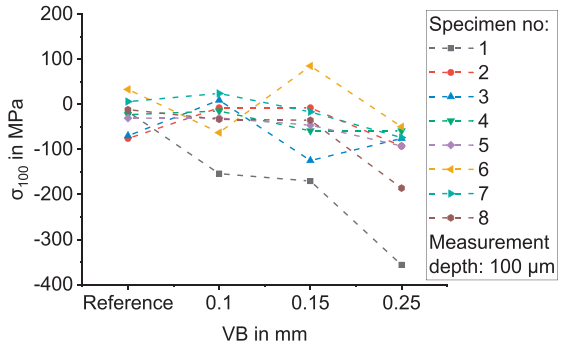

Fig. 37. Axial compressive residual stress at a measurement depth of 100 µm.

7. Applications of surface conditioning

7.1. Modeling the surface hardening when cryogenic turning austenitic steal using an ML-based model (CRC 926)

Metastable, austenitic steels inhibit a favorable combination of strength and ductility as well as an excellent corrosion resistance, which is why they are widely used in industry. If these steels are cryogenically machined, a surface hardening is achievable via strain hardening in superposition with a deformation-induced phase transformation from γ-austenite into ε- and α'-martensite [19]. To promote these effects and therefore realize a sufficient surface hardening, low temperatures as well as high mechanical loads have to be provided by the cryogenic machining process [111]. By applying surface hardening via cryogenic turning, the fatigue strength [24] as well as wear resistance [77] of the austenitic steel could be improved.

However, in order to properly tailor the cryogenic process to realize surface layer properties specified to certain application requirements, the causal correlations between the input parameters, the occurring thermo-mechanical loads and the resulting surface integrity have to be understood. These causal relationships have been investigated within the CRC 926 to develop a ML-based model that can predict the martensite content within the surface layer in dependence of the cryogenic turning process (see Fig. 38). To model the resulting martensite, *a priori* knowledge is needed on how the cutting process influences the occurring thermo-mechanical loads which lead to the martensitic phase transformation. This knowledge was gathered via cutting experiments which characterized the influence of cutting parameters [111,112,169], tool properties (cutting edge radius r_β, rake angle γ_β, K-factor K, coating [110–112,168]), and cooling strategy (precooling, CO_2 mass flow [111,169]) on the occurring forces and resulting temperatures during cutting. Using the measured forces and temperatures as input data, three algorithms (SVM, ANN, RF) were used to predict the resulting martensite content ζ. A total of 55 data sets were used for training and testing the ML algorithms with an 80 to 20 ratio respectively. As a result, SVM delivered the best accuracy (R^2 = 99.21%), followed by ANN (R^2 = 88.62%) and RF (R^2 = 70.78%) in predicting the resulting martensite content [83].

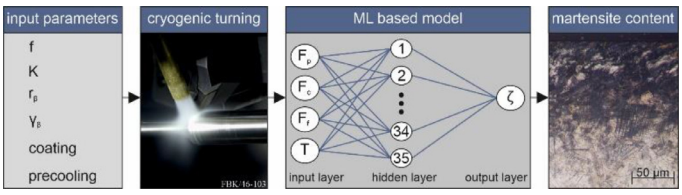

Fig. 38. Depiction of the ML-based model to predict the martensite content according to [111].

Cryogenic turning of metastable austenitic steel allows the integration of process hardening into the form-shaping process. With the investigated correlations and the trained ML model, it is now possible to determine the martensite content and therefore surface hardness by means of an indirect measurement of the process forces and the temperatures. Therefore, process monitoring allows the estimation of changes of the martensite content due to a variation of the thermo-mechanical loads, for example due to tool wear. Future development can focus on the implementation of a soft, sensor-based process control that can be used in industry to ensure the robust machining of workpieces with defined surface layer properties.

7.2. In-process prediction of surface quality during cryogenic hard turning using soft sensors (PP 2086)

In cryogenic hard turning of quenched and tempered 100Cr6, the application behavior can also be optimized by targeted surface conditioning. This is due to metallurgical changes in the surface layer (e.g., grain refinement) and the introduction of favorable residual compressive stresses [269,277]. To properly design this process of surface conditioning, the causal relationships between the input parameters of the cutting process (cutting speed, feed, depth of cut, mass flow of the cryogenic coolant) and the resulting surface layer properties have to be understood. These causal relationships have so far been investigated within the PP 2086 and are well understood [13,21]. However, during turning, especially within industrial applications, several disturbances like progressing tool wear, altering cutting edge preparations or changes of the batch occur, which have an influence on the process characteristics and therefore the resulting surface layer properties. While their respective influence on the surface layer properties has also been investigated [87], these occurring disturbances still have to be monitored during the process in order to control the surface conditioning process. This is undertaken indirectly by measuring the forces, temperatures, and acoustic emissions, which occur during cutting. In addition, an opto-pneumatic sensor was developed and implemented, allowing for an in-process measurement of the surface topography [264]. These in-process measurements are used as an input for a developed soft sensor [263]. This soft sensor utilized models derived from the causal relations observed by the experimental data to predict the resulting surface layer properties in relation to the occurring process characteristics. This allows for an in-situ prediction of the surface condition that is manufactured. As a next step, a process control has to be implemented into the soft sensor. This will allow for automated adjustments of the cutting process independence of the in-process monitoring. If an action is required, the soft sensor will choose to adjust a variable which is easy to vary and has the biggest impact. For example, when the required values of residual stresses in the surface area cannot be reached anymore without altering the control variables, the soft sensor will choose to raise the mass flow of coolant, because the models show the highest impact on the residual stresses. A schematic depiction of this process control is given in Fig. 39.

7.3. In-process monitoring and adaptive process control of surface integrity during grinding (PP 2086)

During grinding of hardened steels, the component experiences a thermo-mechanical load that leads to a change in the surface layer state. In case of an incorrect process design, e.g., material-specific critical temperatures can be exceeded to such an extent that damage such as tensile residual stresses and tempering or even rehardening zones occur. Generally, the occurrence of these unwanted modifications is referred to as grinding burn and acts as a thermal process limit [165].

Please cite this article as: V. Schulze et al., Surface conditioning in cutting and abrasive processes, CIRP Annals - Manufacturing Technology (2024), https://doi.org/10.1016/j.cirp.2024.05.004

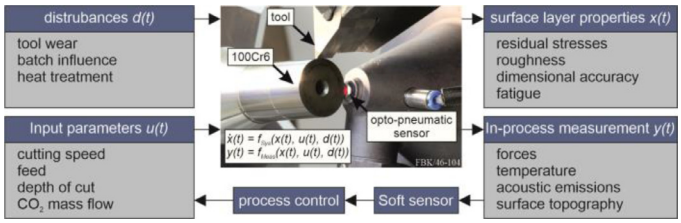

Fig. 39. Schematic depiction of the process control for surface conditioning during hard turning of 100Cr6.

To detect grinding burn, industry still relies on subjective methods such as nital etching or destructive testing methods. In addition, in many cases, no measurements of the modification can be provided [132]. Analytical-empirical models and micromagnetic measurement methods are suitable for a non-destructive detection of grinding burn and quantitative surface layer analysis [103,105]. Both approaches combined in a soft sensor signal enable an adjustment of the process towards a favorable surface layer state by a process-oriented control between grinding cycles.

Based on an empirical model in surface layer modification charts presented in Section 3.4 (c.f. Fig. 11), a thermal process limit for avoiding tempering zones is implemented depending on the specific grinding power Pc'' and the contact time Δt [103,105]. The grinding power can be measured directly or calculated by measuring process forces. If the critical limit is exceeded, an onset of grinding burn occurs. Therefore, the soft sensor adapts the radial feed speed v_{fr} or workpiece speed v_w in the process control or even carries out a dressing process to recondition the grinding wheel. Since critical tensile residual stresses can already occur before the onset of tempering zones, the micromagnetic measurement of Barkhausen noise is also used. For this purpose, an experimental setup for in-process Barkhausen noise measurement using 3MA technology was developed in order to be able to expand the soft sensor in the future [123].

8. Summary and future research

This keynote paper has proposed a concept for a paradigm change in machining, which allows the combination of the classical demand of geometry justification with the new demand of surface layer adjustment and therefore the control of workpiece functional properties. This is called surface conditioning and combines in-process measurement of changes in the process with models interpreting these changes as influence on the surface layer properties. If these so-called soft sensors are used in active control of machining processes, the adjustment of the functional properties as described is affordable.

At the beginning, it is shown how surface integrity or surface engineering is established today and which variety of surface layer states can be induced in machining. Additionally, mechanism-oriented descriptions of major effects on the surface layer are described according to the concept of process signatures and their correlations with functional properties like fatigue, tribological properties, and corrosion resistance are referred to.

In-process measurement methods, used in surface conditioning may be referring to topography and based on optical sensors. Acoustic emission, temperature, cutting force, micromagnetic Barkhausen noise, and eddy current sensors can indirectly measure surface layer properties, which may be related to microstructure and/or residual stresses analysis. They may be used in-process in contrast to more precise and time consuming techniques like X-ray diffraction, electron backscattered diffraction, micro/nano indentation, and Raman spectroscopy. Combining in-process sensors can provide comprehensive surface integrity measurement.

In the field of modeling surface layer effects in machining operations, physically based models of mechanical behavior and loads as well as thermal loads due to processing are used. Special models like dynamical recrystallization and Helmholtz-free energy description of phase changes are available and well established. The use of machine learning-based models is increasing to optimize the processes and predict surface integrity. They require data acquisition from the in-process sensors mentioned before, preprocessing, feature extraction, and selection of the appropriate algorithm. Here, support vector machines and artificial neural networks are commonly used for prediction. Finally, grey-box/hybrid models which combine physics-based and machine learning-based models are emerging to improve prediction accuracy. All these models are applicable as a basis for soft sensors when combined with in-process measurement in cutting and abrasive processes. Using these, a control of surface layer properties is possible using concepts of active, real time control within the machine tool. A joint round robin test on residual stress adjustment showed the different approaches available and also the great challenges remaining in the conditioning of surface layer properties. Besides some organizational issues, this was especially caused by difficulties in accessing machine tool control and establishing active control loops implemented outside the machine tool itself. Specifically, the identification of control parameters and the previous validation of thorough models interpreting the in-process sensor data still impose questions on the intensity of necessary reactions in the process. In case of ML-supported strategies, this may also be caused by the small amount of data used in the training phase. In total, it needs to be stated that many of the challenges and limitations encountered during the CIRP Collaborative Working Group on Surface Integrity and Functional Performance of Components which lead to the STC S keynote 2011 [122] have basically not been overcome and are still valid. Substantial developments are necessary in order to achieve a successful compensation of disturbances in technical cutting operations. Nevertheless, a limited number of first positive applications of the concepts described in relevant processes exists and examples are given at the end of the paper.

In conclusion, surface conditioning by combining in-process sensors with soft sensors models and their use in active process control is a promising but still challenging concept to be applicable for future machining applications. Besides single items regarding sensors and models, a comprehensive approach ensuring access to the machine tool control and establishing an external active control is missing. Even in an elaborated situation, a lot of data for identification of the soft sensor model part and the control parameters is necessary to eventually yield to an economic perspective in large-scale production. However, there clearly is a high potential in combining the adjustment of workpiece geometry with the control of the surface layer state and therefore of the functional properties.

Declaration of competing interest

The authors declare that they have no known competing financial interests or personal relationships that could have appeared to influence the work reported in this paper.

CRediT authorship contribution statement

Volker Schulze: Writing – review & editing, Writing – original draft, Visualization, Resources, Project administration, Methodology, Investigation, Data curation, Conceptualization. **Jan Aurich:** Writing – review & editing, Writing – original draft, Visualization, Resources, Project administration, Methodology, Investigation, Data curation, Conceptualization. **I.S. Jawahir:** Writing – review & editing, Writing

Please cite this article as: V. Schulze et al., Surface conditioning in cutting and abrasive processes, CIRP Annals - Manufacturing Technology (2024), https://doi.org/10.1016/j.cirp.2024.05.004

– original draft, Visualization, Resources, Project administration, Methodology, Investigation, Data curation, Conceptualization. **Bernhard Karpuschewski:** Writing – review & editing, Writing – original draft, Visualization, Resources, Project administration, Methodology, Investigation, Data curation, Conceptualization. **Jiwang Yan:** Writing – review & editing, Writing – original draft, Visualization, Resources, Project administration, Methodology, Investigation, Data curation, Conceptualization.

Acknowledgements

The support of Walter AG in providing the tools, Eckehard Müller for the X-ray residual stress analyses and of all the contributors to the round robin test is appreciated by the authors. They also would like to express their sincere thanks to James Caudill, Kevin Gutzeit, Lars Langenhorst, Jannik Schwalm, and Weihai Huang for their fruitful contribution, detailed discussion, and involvement in the preparation of this paper.

References

[1] Abboud E, Shi B, Attia H, Thomson V, Mebrahtu Y (2013) Finite Element-based Modeling of Machining-induced Residual Stresses in Ti-6Al-4V under Finish Turning Conditions. *Procedia CIRP* 8:63–68.
[2] Aben H, Ainola L, Anton J (2000) Integrated Photoelasticity For Nondestructive Residual Stress Measurement In Glass. *Optics and Lasers in Engineering* 33(1): 49–64.
[3] Abu-Nabah BA, Nagy PB (2007) High-Frequency Eddy Current Conductivity Spectroscopy For Residual Stress Profiling In Surface-Treated Nickel-Base Superalloys. *NDT & E International* 40(5):405–418.
[4] Agarwal S, Venkateswara Rao P (2010) Modeling And Prediction Of Surface Roughness In Ceramic Grinding. *International Journal of Machine Tools and Manufacture* 50(12):1065–1076.
[5] Aghdam BH, Vahdati M, Sadeghi MH (2015) Vibration-Based Estimation Of Tool Major Flank Wear In A Turning Process Using ARMA Models. *International Journal of Advanced Manufacturing Technology* 76(9):1631–1642.
[6] Agrawal S, Joshi SS (2013) Analytical Modelling Of Residual Stresses In Orthogonal Machining Of AISI4340 Steel. *Journal of Manufacturing Processes* 15(1): 167–179.
[7] Aida H, Takeda H, Doi T (2021) Analysis Of Mechanically Induced Subsurface Damage And Its Removal By Chemical Mechanical Polishing For Gallium Nitride Substrate. *Precision Engineering* 67:350–358.
[8] Akcan S, Shah WS, Moylan SP, Chandrasekar S, Chhabra PN, Yang HTY (2002) Formation Of White Layers In Steels By Machining And Their Characteristics. *Metallurgical and Materials Transactions A* 33(4):1245–1254.
[9] Akhavan Niaki F, Mears L (2017) A Comprehensive Study On The Effects Of Tool Wear On Surface Roughness, Dimensional Integrity And Residual Stress In Turning IN718 Hard-To-Machine Alloy. *Journal of Manufacturing Processes* 30:268–280.
[10] Albertelli P, Goletti M, Torta M, Salehi M, Monno M (2016) Model-Based Broadband Estimation Of Cutting Forces And Tool Vibration In Milling Through In-Process Indirect Multiple-Sensors Measurements. *International Journal of Advanced Manufacturing Technology* 82(5-8):779–796.
[11] Alonso U, Ortega N, Sanchez JA, Pombo I, Izquierdo B, Plaza S (2015) Hardness Control Of Grind-Hardening And Finishing Grinding By Means Of Area-Based Specific Energy. *International Journal of Machine Tools and Manufacture* 88: 24–33.
[12] Altendeitering M, Dübler S (2020) Scalable Detection of Concept Drift: A Learning Technique Based on Support Vector Machines. *Procedia Manufacturing* 51:400–407.
[13] Ankener W, Uebel J, Basten S, Smaga M, Kirsch B, Seewig J, Aurich JC, Beck T (2020) Influence Of Different Cooling Strategies During Hard Turning Of AISI 52100 – Part II: Characterization Of The Surface And Near Surface Microstructure Morphology. *Procedia CIRP* 87:119–124.
[14] Argibay N, Chandross M, Cheng S, Michael JR (2017) Linking Microstructural Evolution And Macro-Scale Friction Behavior In Metals. *Journal of Materials Science* 52(5):2780–2799.
[15] Arinez JF, Chang Q, Gao RX, Xu C, Zhang J (2020) Artificial Intelligence in Advanced Manufacturing: Current Status and Future Outlook. *Journal of Manufacturing Science and Engineering* 142(11).
[16] Arrazola PJ, Özel T, Umbrello D, Davies M, Jawahir IS (2013) Recent Advances In Modelling Of Metal Machining Processes. *CIRP Annals* 62(2):695–718.
[17] Aslan D, Budak E (2015) Surface Roughness And Thermo-Mechanical Force Modeling For Grinding Operations With Regular And Circumferentially Grooved Wheels. *Journal of Materials Processing Technology* 223:75–90.
[18] Aurich JC, Biermann D, Blum H, Brecher C, Carstensen C, Denkena B, Klocke F, Kröger M, Steinmann P, Weinert K (2009) Modelling And Simulation Of Process: Machine Interaction In Grinding. *Production Engineering* 3(1):111–120.
[19] Aurich JC, Mayer P, Kirsch B, Eifler D, Smaga M, Skorupski R (2014) Characterization Of Deformation Induced Surface Hardening During Cryogenic Turning Of AISI 347. *CIRP Annals* 63(1):65–68.
[20] Ayvaz S, Alpay K (2021) Predictive Maintenance System For Production Lines In Manufacturing: A Machine Learning Approach Using Iot Data In Real-Time. *Expert Systems with Applications* 173:114598.
[21] Basten S, Kirsch B, Ankener W, Smaga M, Beck T, Uebel J, Seewig J, Aurich JC (2020) Influence Of Different Cooling Strategies During Hard Turning of AISI 52100 - Part I: Thermo-Mechanical Load, Tool Wear, Surface Topography And Manufacturing Accuracy. *Procedia CIRP* 87:77–82.
[22] Bhavsar H, Panchal Mahesh, H (2012) A Review On Support Vector Machine For Data Classification. *International Journal of Advanced Research in Computing Engineering & Technology* 1(10):185–189.
[23] Blau PJ (1991) Running-in: Art or Engineering? *Journal of Materials Engineering* 13(1):47–53.
[24] Boemke A, Smaga M, Beck T (2018) Influence Of Surface Morphology On The Very High Cycle Fatigue Behavior Of Metastable And Stable Austenitic Cr-Ni Steels. MATEC Web Conf. 165:20008.
[25] Bomas H, Schleicher M (2005) Application Of The Weakest-Link Concept To The Endurance Limit Of Notched And Multiaxially Loaded Specimens Of Carburized Steel 16MnCrS5. *Fatigue & Fracture of Engineering Materials and Structures* 28 (11):983–995.
[26] Bosheh SS, Mativenga PT (2006) White Layer Formation In Hard Turning Of H13 Tool Steel At High Cutting Speeds Using CBN Tooling. *International Journal of Machine Tools and Manufacture* 46(2):225–233.
[27] Botko F, Zajac J, Czan A, Radchenko S, Lehocka D, Duplak J (2019) Influence of Residual Stress Induced in Steel Material on Eddy Currents Response Parameters. in Gapiński B, Szostak M, Ivanov V, (Eds.) *Advances in Manufacturing II*, Springer International Publishing, Cham, 551–560.
[28] Böttger D, Stampfer B, Gauder D, Straß B, Häfner B, Lanza G, Schulze V, Wolter B (2020) Concept For Soft Sensor Structure For Turning Processes Of AISI4140. *tm - Technisches Messen* 87(12):745–756.
[29] Brinksmeier E, Aurich JC, Govekar E, Heinzel C, Hoffmeister H-W, Klocke F, Peters J, Rentsch R, Stephenson DJ, Uhlmann E, Weinert K, Wittmann M (2006) Advances in Modeling and Simulation of Grinding Processes. *CIRP Annals* 55 (2):667–696.
[30] Brinksmeier E, Gläbe R, Klocke F, Lucca DA (2011) Process Signatures – an Alternative Approach to Predicting Functional Workpiece Properties. *Procedia Engineering* 19:44–52.
[31] Brinksmeier E, Heinzel C, Garbrecht M, Sölter J, Reucher G (2011) Residual Stresses In High Speed Turning Of Thin-Walled Cylindrical Workpieces. *International Journal of Automation Technology* .
[32] Brinksmeier E, Klocke F, Lucca DA, Sölter J, Meyer D (2014) Process Signatures – A New Approach to Solve the Inverse Surface Integrity Problem in Machining Processes. *Procedia CIRP* 13:429–434.
[33] Brinksmeier E, Meyer D, Heinzel C, Lübben T, Sölter J, Langenhorst L, Frerichs F, Kämmler J, Kohls E, Kuschel S (2018) Process Signatures - The Missing Link to Predict Surface Integrity in Machining. *Procedia CIRP* 71:3–10.
[34] Brinksmeier E, Reese S, Klink A, Langenhorst L, Lübben T, Meinke M, Meyer D, Riemer O, Sölter J (2018) Underlying Mechanisms for Developing Process Signatures in Manufacturing. *Nanomanufacturing and Metrology* 1(4):193–208.
[35] Brown M, Ghadbeigi H, Crawforth P, M'Saoubi R, Mantle A, McGourlay J, Wright D (2020) Non-Destructive Detection Of Machining-Induced White Layers In Ferromagnetic Alloys. *Procedia CIRP* 87:420–425.
[36] Brown M, Pieris D, Wright D, Crawforth P, M'Saoubi R, McGourlay J, Mantle A, Patel R, Smith RJ, Ghadbeigi H (2021) Non-Destructive Detection Of Machining-Induced White Layers Through Grain Size And Crystallographic Texture-Sensitive Methods. *Materials & Design* 200:109472.
[37] Brown M, Wright D, M'Saoubi R, McGourlay J, Wallis M, Mantle A, Crawforth P, Ghadbeigi H (2018) Destructive And Non-Destructive Testing Methods For Characterization And Detection Of Machining-Induced White Layer: A Review Paper. *CIRP Journal of Manufacturing Science and Technology* 23:39–53.
[38] Buchkremer S, Klocke F (2017) Compilation Of A Thermodynamics Based Process Signature For The Formation Of Residual Surface Stresses In Metal Cutting. *Wear* 376-377(2):1156–1163.
[39] Burges CJ (1998) A Toutorial on Support Vector Machines for Pattern Recognition. *Data Mining and Knowledge Discovery* 2(2):121–167.
[40] Cabrini M, Cigada A, Rondelli G, Vicentini B (1997) Effect Of Different Surface Finishing And Of Hydroxyapatite Coatings On Passive And Corrosion Current Of Ti6Al4V Alloy In Simulated Physiological Solution. *Biomaterials* 18 (11):783–787.
[41] Cai J, Luo J, Wang S, Yang S (2018) Feature Selection In Machine Learning: A New Perspective. *Neurocomputing* 300:70–79.
[42] Capello E (2005) Residual Stresses In Turning. *Journal of Materials Processing Technology* 160(2):221–228.
[43] Capello E (2006) Residual Stresses In Turning. *Journal of Materials Processing Technology* 172(3):319–326.
[44] Caruso S, Umbrello D, Outeiro JC, Filice L, Micari F (2011) An Experimental Investigation of Residual Stresses in Hard Machining of AISI 52100 Steel. *Procedia Engineering* 19:67–72.
[45] Caudill J (2019) *Enhanced Surface Integrity With Thermally Stable Residual Stress Fields and Nanostructures in Cryogenic Processing of Titanium Alloy Ti-6Al-4V*, PhD Dissertation, University of Kentucky.
[46] Chandrashekar G, Sahin F (2014) A Survey On Feature Selection Methods. *Computers & Electrical Engineering* 40(1):16–28.

[47] Chen G, Caudill J, Ren C, Jawahir IS (2022) Numerical Modeling of Ti-6Al-4V Alloy Orthogonal Cutting Considering Microstructure Dependent Work Hardening And Energy Density-Based Failure Behaviors. *Journal of Manufacturing Processes* 82:750–764.
[48] Chen H, Tang J, Zhou W (2013) Modeling And Predicting Of Surface Roughness For Generating Grinding Gear. *Journal of Materials Processing Technology* 213 (5):717–721.
[49] Chen X, Han Z, Li X, Lu K (2016) Lowering Coefficient Of Friction In Cu Alloys With Stable Gradient Nanostructures. *Science Advances* 2(12): e1601942.
[50] Chen Z, Peng RL, Zhou J, M'Saoubi R, Gustafsson D (2019) Effect Of Machining Parameters On Cutting Force And Surface Integrity When High-Speed Turning AD 730™ With PCBN Tools. *International Journal of Advanced Manufacturing Technology* (100):2601–2615.
[51] Cho D-H, Lee S-A, Lee Y-Z (2012) Mechanical Properties and Wear Behavior of the White Layer. *Tribology Letters* 45(1):123–129.
[52] Choi TJ, Subrahmanya N, Li H, Shin YC (2008) Generalized Practical Models Of Cylindrical Plunge Grinding Processes. *International Journal of Machine Tools and Manufacture* 48(1):61–72.
[53] Chou Y, Evans CJ (1999) White Layers And Thermal Modeling Of Hard Turned Surfaces. *International Journal of Machine Tools and Manufacture* 39(12):1863–1881.
[54] Choudhury SK, Rath S (2000) In-Process Tool Wear Estimation In Milling Using Cutting Force Model. *Journal of Materials Processing Technology* 99(1):113–119.
[55] Clavier F, Valiorgue F, Courbon C, Dumas M, Rech J, van Robaeys A, Lefebvre F, Brosse A, Karaouni H (2020) Impact Of Cutting Tool Wear On Residual Stresses Induced During Turning Of A 15-5 PH Stainless Steel. *Procedia CIRP* 87:107–112.
[56] Ćojbašić Ž, Petković D, Shamshirband S, Tong CW, Ch S, Janković P, Dučić N, Baralić J (2016) Surface Roughness Prediction By Extreme Learning Machine Constructed With Abrasive Water Jet. *Precision Engineering* 43:86–92.
[57] Dahlman P, Gunnberg F, Jacobson M (2004) The Influence Of Rake Angle, Cutting Feed And Cutting Depth On Residual Stresses In Hard Turning. *Journal of Materials Processing Technology* .
[58] Denguir LA, Outeiro JC, Fromentin G, Vignal V, Besnard R (2017) A Physical-Based Constitutive Model For Surface Integrity Prediction In Machining of OFHC Copper. *Journal of Materials Processing Technology* 248:143–160.
[59] Deris AM, Zain AM, Sallehuddin R (2011) Overview of Support Vector Machine in Modeling Machining Performances. *Procedia Engineering* 24:308–312.
[60] Ding H, Shin YC (2013) Multi-Physics Modeling And Simulations Of Surface Microstructure Alteration In Hard Turning. *Journal of Materials Processing Technology* 213(6):877–886.
[61] Dong P, Peng H, Cheng X, Xing Y, Tang W, Zhou X (2019) Semi-Empirical Prediction of Residual Stress Profiles in Machining IN718 Alloy Using Bimodal Gaussian Curve. *Materials* 12(23).
[62] Du C, Ho CL, Kaminski J (2021) Prediction Of Product Roughness, Profile, And Roundness Using Machine Learning Techniques For A Hard Turning Process. *Advances in Manufacturing* 9(2):206–215.
[63] Du Preez A, Oosthuizen GA (2019) Machine Learning In Cutting Processes As Enabler For Smart Sustainable Manufacturing. *Procedia Manufacturing* 33:810–817.
[64] Duarte B, Saraiva PM, Pantelides CC (2004) Combined Mechanistic and Empirical Modelling. *International Journal of Chemical Reactor Engineering* 2(1).
[65] Dumas M, Fabre D, Valiorgue F, Kermouche G, van Robaeys A, Girinon M, Brosse A, Karaouni H, Rech J (2021) 3D Numerical Modelling Of Turning-Induced Residual Stresses – A Two-Scale Approach Based On Equivalent Thermo-Mechanical Loadings. *Journal of Materials Processing Technology* 297:117274.
[66] Ee KC, Dillon OW, Jawahir IS (2005) Finite Element Modeling Of Residual Stresses In Machining Induced By Cutting Using A Tool With Finite Edge Radius. *International Journal of Mechanical Sciences* 47(10):1611–1628.
[67] Elsheikh AH, Muthuramalingam T, Shanmugan S, Mahmoud Ibrahim AM, Ramesh B, Khoshaim AB, Moustafa EB, Bedairi B, Panchal H, Sathyamurthy R (2021) Fine-Tuned Artificial Intelligence Model Using Pigeon Optimizer For Prediction Of Residual Stresses During Turning Of Inconel 718. *Journal of Materials Research and Technology* 15:3622–3634.
[68] Erbacher T, Wanner A (2008) X-Ray Analysis Of Steep Residual Stress Gradients: The 2θ-Derivative Method. *International Journal of Materials Research* 99 (10):1071–1078.
[69] Fatemi A, Socie DF (1988) A Critical Plane Approach To Multiaxial Fatigue Damage Including Out-Of-Phase Loading. *Fatigue & Fracture of Engineering Materials and Structures* 11(3):149–165.
[70] Field M, Kahles JF (1964) The Surface Integrity of Machined and Ground High Strength Steels. *DMIC Report* 210:54–77.
[71] Field M, Kahles JF (1971) Review Of Surface Integrity Of Machined Components. *CIRP Annals* 20(2):153–163.
[72] Field M, Koster W (1978) Optimizing Grinding Parameters To Combine High Productivity With High Surface Integrity. *CIRP Annals* 27(1):523–526.
[73] Fredj NB, Amamou R (2006) Ground Surface Roughness Prediction Based Upon Experimental Design And Neural Network Models. *International Journal of Advanced Manufacturing Technology* 31(1-2):24–36.
[74] Frerichs F, Lübben T (2018) Development of Process Signatures for Manufacturing Processes with Thermal Loads without and with hardening. *Procedia CIRP* 71:418–423.
[75] Fricke LV, Nguyen HN, Breidenstein B, Denkena B, Dittrich M-A, Maier HJ, Zaremba D (2020) Generation Of Tailored Subsurface Zones In Steels Containing Metastable Austenite By Adaptive Machining And Validation By Eddy Current Testing. *tm - Technisches Messen* 87(11):704–713.
[76] Fricke LV, Nguyen HN, Breidenstein B, Zaremba D, Maier HJ (2021) Eddy Current Detection of the Martensitic Transformation in AISI304 Induced upon Cryogenic Cutting. *Steel Research International* 92(1):2000299.
[77] Frölich D, Magyar B, Sauer B, Mayer P, Kirsch B, Aurich JC, Skorupski R, Smaga M, Beck T, Eifler D (2015) Investigation Of Wear Resistance Of Dry And Cryogenic Turned Metastable Austenitic Steel Shafts And Dry Turned And Ground Carburized Steel Shafts In The Radial Shaft Seal Ring System. *Wear* 328-329:123–131.
[78] Fukuhara Y, Suzuki S, Sasahara H (2018) Real-Time Grinding State Discrimination Strategy By Use Of Monitor-Embedded Grinding Wheels. *Precision Engineering* 51:128–136.
[79] Furutani K, Ohguro N, Hieu NT, Nakamura T (2002) In-Process Measurement Of Topography Change Of Grinding Wheel By Using Hydrodynamic Pressure. *International Journal of Machine Tools and Manufacture* 42(13):1447–1453.
[80] Gao W, Haitjema H, Fang FZ, Leach RK, Cheung CF, Savio E, Linares JM (2019) On-Machine And In-Process Surface Metrology For Precision Manufacturing. *CIRP Annals* 68(2):843–866.
[81] García-Martín J, Gómez-Gil J, Vázquez-Sánchez E (2011) Non-Destructive Techniques Based on Eddy Current Testing. *Sensors* 11(3):2525–2565.
[82] Genzel C, Stock C, Reimers W (2004) Application Of Energy-Dispersive Diffraction To The Analysis Of Multiaxial Residual Stress Fields In The Intermediate Zone Between Surface And Volume. *Materials Science and Engineering: A* 372 (1):28–43.
[83] Glatt M, Hotz H, Kölsch P, Mukherjee A, Kirsch B, Aurich JC (2021) Predicting The Martensite Content Of Metastable Austenitic Steels After Cryogenic Turning Using Machine Learning. *International Journal of Advanced Manufacturing Technology* 115(3):749–757.
[84] Godet M (1984) The Third-Body Approach: A Mechanical View Of Wear. *Wear* 100(1-3):437–452.
[85] González G, Plogmeyer M, Schoop J, Bräuer G, Schulze V (2023) In-Situ Characterization Of Tool Temperatures Using In-Tool Integrated Thermoresistive Thin-Film Sensors. *Production Engineering* 17(2):319–328.
[86] Gonzalez Zelaya CV (2019) Towards Explaining the Effects of Data Preprocessing on Machine Learning. *2019 IEEE 35th International Conference on Data Engineering: 8-11 April 2019, Macau, SAR, China proceedings*, IEEE, Piscataway, NJ, 2086–2090.
[87] Grossmann F, Basten S, Kirsch B, Ankener W, Smaga M, Beck T, Uebel J, Seewig J, Aurich JC (2022) Predictive Modelling Of Cryogenic Hard Turning Of AISI 52100 Based On Response Surface Methodology For The Use In Soft Sensors. *Procedia CIRP* 108:270–275.
[88] Grzesik W, Kruszynski B, Ruszaj A (2010) *Surface Integrity of Machined Surfaces*, Springer.
[89] Grzesik W, Małecka J, Kwaśny W (2020) Identification Of Oxidation Process Of TiALN Coatings Versus Heat Resistant Aerospace Alloys Based On Diffusion Couples And Tool Wear Tests. *CIRP Annals* 69(1):41–44.
[90] Gu X, Zhao Q, Wang H, Xue J, Guo B (2019) Fundamental Study On Damage-Free Machining Of Sapphire: Revealing Damage Mechanisms Via Combining Elastic Stress Fields And Crystallographic Structure. *Ceramics International* 45 (16):20684–20696.
[91] Guba N, Heinzel J, Heinzel C, Karpuschewski B (2020) Grinding Burn Limits: Generation Of Surface Layer Modification Charts For Discontinuous Profile Grinding With Analogy Trials. *CIRP Journal of Manufacturing Science and Technology* 31:99–107.
[92] Gunnberg F, Escursell M, Jacobson M (2006) The Influence Of Cutting Parameters On Residual Stresses And Surface Topography During Hard Turning Of 18MnCr5 Case Carburised Steel. *Journal of Materials Processing Technology* 174(1-3): 82–90.
[93] Guo J, FU H, Pan B, Kang R (2021) Recent Progress Of Residual Stress Measurement Methods: A Review. *Chinese Journal of Aeronautics* 34(2):54–78.
[94] Guo J, Wang B, He Z-X, Pan B, Du D-X, Huang W, Kang R-K (2021) A Novel Method For Workpiece Deformation Prediction By Amending Initial Residual Stress Based On SVR-GA. *Advances in Manufacturing* 9(4):483–495.
[95] Guo YB, Ammula SC (2005) Real-Time Acoustic Emission Monitoring For Surface Damage In Hard Machining. *International Journal of Machine Tools and Manufacture* 45(14):1622–1627.
[96] Guo YB, Anurag S, Jawahir IS (2009) A Novel Hybrid Predictive Model And Validation Of Unique Hook-Shaped Residual Stress Profiles In Hard Turning. *CIRP Annals* 58(1):81–84.
[97] Guo YB, Li W, Jawahir IS (2009) Surface Integrity Characterization And Prediction In Machining Of Hardened And Difficult-To-Machine Alloys: A State-Of-Art Research Review And Analysis. *Machining Science and Technology* 13(4):437–470.
[98] Guo YB, Liu CR (2002) 3D FEA Modeling of Hard Turning. *Journal of Manufacturing Science and Engineering* 124(2):189–199.
[99] Guo YB, Waikar RA (2009) An Experimental Study on the Effect of Machining-Induced White Layer on Frictional and Wear Performance at Dry and Lubricated Sliding Contact. *Tribology Transactions* 53(1):127–136.
[100] Guo YB, Warren AW, Hashimoto F (2010) The Basic Relationships Between Residual Stress, White Layer, And Fatigue Life Of Hard Turned And Ground Surfaces In Rolling Contact. *CIRP Journal of Manufacturing Science and Technology* 2 (2):129–134.
[101] Güray A, Böttger D, González G, Stamer F, Lanza G, Wolter B, Schulze V (2023) Modeling The Effect Of Workpiece Temperature On Micromagnetic High-Speed-3MA-Testing In Case Of AISI 4140. *Procedia CIRP* 117:133–138.
[102] Heinzel C, Bleil N (2007) The Use of the Size Effect in Grinding for Work-hardening. *CIRP Annals* 56(1):327–330.

[103] Heinzel C, Heinzel J, Guba N, Hüsemann T (2021) Comprehensive Analysis Of The Thermal Impact And Its Depth Effect In Grinding. *CIRP Annals* 70(1):289–292.
[104] Heinzel C, Sölter J, Jermolajev S, Kolkwitz B, Brinksmeier E (2014) A Versatile Method to Determine Thermal Limits in Grinding. *Procedia CIRP* 13:131–136.
[105] Heinzel J, Jedamski R, Rößler M, Karpuschewski B, Epp J, Dix M (2022) Hybrid Approach To Evaluate Surface Integrity Based On Grinding Power And Barkhausen Noise. *Procedia CIRP* 108:489–494.
[106] Heinzel J, Sackmann D, Karpuschewski B (2019) Micromagnetic Analysis of Thermally Induced Influences on Surface Integrity Using the Burning Limit Approach. *Journal of Manufacturing and Materials Processing* 3(4).
[107] Herzenstiel P, Aurich JC (2010) CBN-Grinding Wheel With Defined Grain Pattern - Extensive Numerical And Experimental Studies. *Machining Science and Technology* 14(3):301–322.
[108] Holmberg J, Wretland A, Hammersberg P, Berglund J, Suárez A, Beno T (2021) Surface Integrity Investigations For Prediction Of Fatigue Properties After Machining Of Alloy 718. *International Journal of Fatigue* 144:106059.
[109] Hong T, Nagumo M (1997) Effect Of Surface Roughness On Early Stages Of Pitting Corrosion Of Type 301 Stainless Steel. *Corrosion Science* 39(9):1665–1672.
[110] Hotz H, Kirsch B (2020) Influence Of Tool Properties On Thermomechanical Load And Surface Morphology When Cryogenically Turning Metastable Austenitic Steel AISI 347. *Journal of Manufacturing Processes* 52:120–131.
[111] Hotz H, Kirsch B, Aurich JC (2021) Impact Of The Thermomechanical Load On Subsurface Phase Transformations During Cryogenic Turning Of Metastable Austenitic Steels. *Journal of Intelligent Manufacturing* 32(3):877–894.
[112] Hotz H, Kirsch B, Becker S, von Harbou E, Müller R, Aurich JC (2018) Modification Of Surface Morphology During Cryogenic Turning Of Metastable Austenitic Steel AISI 347 At Different Parameter Combinations With Constant CO2 Consumption Per Cut. *Procedia CIRP* 77:207–210.
[113] Hu KX, Chandra A (1993) A Fracture Mechanics Approach to Modeling Strength Degradation in Ceramic Grinding Processes. *Journal of Engineering for Industry* 115(1):73–84.
[114] Hua J, Shivpuri R, Cheng X, Bedekar V, Matsumoto Y, Hashimoto F, Watkins TR (2005) Effect Of Feed Rate, Workpiece Hardness And Cutting Edge On Subsurface Residual Stress In The Hard Turning Of Bearing Steel Using Chamfer+Hone Cutting Edge Geometry. *Materials Science and Engineering: A* 394(1-2):238–248.
[115] Huang W, Yan J (2021) Chip-Free Surface Patterning Of Toxic Brittle Polycrystalline Materials Through Micro/Nanoscale Burnishing. *International Journal of Machine Tools and Manufacture* 162:103688.
[116] Huang W, Yan J (2021) Deformation Behaviour Of Soft-Brittle Polycrystalline Materials Determined By Nanoscratching With A Sharp Indenter. *Precision Engineering* 72:717–729.
[117] Hughes DA, Hansen N (2001) Graded Nanostructures Produced By Sliding And Exhibiting Universal Behavior. *Physical Review Letters* 87(13):135503.
[118] Imad M, Kishawy HA, Yussefian NZ, Hosseini A (2022) Effect Of Cutting Edge Radius When Milling Hardened Steels: A Finite Element Analysis And Surface Integrity Investigation. *Machining Science and Technology* 26(4):571–594.
[119] Jang D, Jung J, Seok J (2016) Modeling And Parameter Optimization For Cutting Energy Reduction In MQL Milling Process. *International Journal of Precision Engineering and Manufacturing-Green Technology* 3(1):5–12.
[120] Jawahir IS, Balaji AK, Rouch KE, Baker JR (2003) Towards Integration Of Hybrid Models For Optimized Machining Performance In Intelligent Manufacturing Systems. *Journal of Materials Processing Technology* 139(1-3):488–498.
[121] Jawahir IS, Balaji AK, Stevenson R (1998) In: *Proc. 1st CIRP International Workshop on Modeling of Machining Operations*, 453.
[122] Jawahir IS, Brinksmeier E, M'Saoubi R, Aspinwall DK, Outeiro JC, Meyer D, Umbrello D, Jayal AD (2011) Surface Integrity In Material Removal Processes: Recent Advances. *CIRP Annals* 60(2):603–626.
[123] Jedamski R, Heinzel J, Karpuschewski B, Epp J (2022) In-Process Measurement of Barkhausen Noise for Detection of Surface Integrity during Grinding. *Applied Sciences* 12(9):4671.
[124] Jedamski R, Heinzel J, Rößler M, Epp J, Eckebrecht J, Gentzen J, Putz M, Karpuschewski B (2020) Potential Of Magnetic Barkhausen Noise Analysis For In-Process Monitoring Of Surface Layer Properties Of Steel Components In Grinding. *tm - Technisches Messen* 87(12):787–798.
[125] Jermolajev S, Brinksmeier E, Heinzel C (2018) Surface Layer Modification Charts For Gear Grinding. *CIRP Annals* 67(1):333–336.
[126] Jiang J, Ge P, Hong J (2013) Study On Micro-Interacting Mechanism Modeling In Grinding Process And Ground Surface Roughness Prediction. *International Journal of Advanced Manufacturing Technology* 67(5-8):1035–1052.
[127] Johnson GR, Cook WH (1983) A Constitutive Model and Data for Metals Subjected to Large Strains, High Strain Rates, and High Temperatures. In: *Proceedings 7th International Symposium on Ballistics, The Hague, 19-21 April*, 541–547.
[128] Junge T, Mehner T, Nestler A, Schubert A, Lampke T (2020) Metrological Characterization Of The Thermomechanical Influence Of The Cross-Section Of The Undeformed Chip On The Surface Properties In Turning Of The Aluminum Alloy EN AW-2017. *tm - Technisches Messen* 87(12):777–786.
[129] Kaelbling LP, Littman ML, Moore AW (1996) Reinforcement Learning: A Survey. *Journal of Artificial Intelligence Research* 4:237–285.
[130] Kannan TDB, kannan GR, Kumar BS, Baskar N (2014) Application of Artificial Neural Network Modeling for Machining Parameters Optimization in Drilling Operation. *Procedia Materials Science* 5:2242–2249.
[131] Karpuschewski B, Kinner-Becker T, Klink A, Langenhorst L, Mayer J, Meyer D, Radel T, Reese S, Sölter J (2022) Process Signatures–Knowledge-Based Approach Towards Function-Oriented Manufacturing. *Procedia CIRP* 108:624–629.
[132] Karpuschewski B, Knoche H-J, Hipke M (2008) Gear Finishing By Abrasive Processes. *CIRP Annals* 57(2):621–640.
[133] Khalid S, Khalil T, Nasreen S (2014) A Survey Of Feature Selection And Feature Extraction Techniques In Machine Learning. *2014 Science and Information Conference (SAI 2014): London, United Kingdom, 27 - 29 August 2014*, IEEE, Piscataway, NJ, 372–378.
[134] Khare SK, Agarwal S (2015) Predictive Modeling of Surface Roughness in Grinding. *Procedia CIRP* 31:375–380.
[135] Khoshaim AB, Elsheikh AH, Moustafa EB, Basha M, Mosleh AO (2021) Prediction Of Residual Stresses In Turning Of Pure Iron Using Artificial Intelligence-Based Methods. *Journal of Materials Research and Technology* 11:2181–2194.
[136] Kim D-H, Kim TJY, Wang X, Kim M, Quan Y-J, Oh JW, Min S-H, Kim H, Bhandari B, Yang I, Ahn S-H (2018) Smart Machining Process Using Machine Learning: A Review and Perspective on Machining Industry. *International Science Journal* 5 (4):555–568.
[137] Kohls E, Heinzel C, Eich M (2021) Evaluation of Hardness and Residual Stress Changes of AISI 4140 Steel Due to Thermal Load during Surface Grinding. *Journal of Manufacturing and Materials Processing* 5(3):73.
[138] Korkmaz ME, Gupta MK, Li Z, Krolczyk GM, Kuntoğlu M, Binali R, Yaşar N, Pimenov DY (2022) Indirect Monitoring Of Machining Characteristics Via Advanced Sensor Systems: A Critical Review. *International Journal of Advanced Manufacturing Technology* 120(11):7043–7078.
[139] Kristensen NR, Madsen H, Jørgensen SB (2004) A Method For Systematic Improvement Of Stochastic Grey-Box Models. *Computers & Chemical Engineering* 28(8):1431–1449.
[140] Kumar A, Ghosh S, Aravindan S (2017) Grinding Performance Improvement Of Silicon Nitride Ceramics By Utilizing Nanofluids. *Ceramics International* 43 (16):13411–13421.
[141] Kusiak A (2017) Smart Manufacturing Must Embrace Big Data. *Nature* 544 (7648):23–25.
[142] Lanza G, Haefner B, Schild L, Berger D, Eschner N, Wagner R, Zaiß M (2019) Inline Measurement Technology and Quality Control. in Gao W, (Ed.) *Metrology*, Springer Singapore, Singapore, 1–35.
[143] Lasaosa A, Gurruchaga K, Arizti F, Martinez-De-Guerenu A (2017) Induction Hardened Layer Characterization and Grinding Burn Detection by Magnetic Barkhausen Noise Analysis. *Journal of Nondestructive Evaluation* 36(2):27.
[144] Lazoglu I, Ulutan D, Alaca BE, Engin S, Kaftanoglu B (2008) An Enhanced Analytical Model For Residual Stress Prediction In Machining. *CIRP Annals* 57(1):81–84.
[145] LeCun Y, Bengio Y, Hinton G (2015) Deep Learning. *Nature* 521(7553):436–444.
[146] Lei MK, Miao WL, Zhu XP, Zhu B, Guo DM (2021) High-Performance Manufacturing Enabling Integrated Design And Processing Of Products: A Case Study Of Metal Cutting. *CIRP Journal of Manufacturing Science and Technology* 35:178–192.
[147] Leonesio M, Fagiano L (2022) A Semi-Supervised Physics-Informed Classifier For Centerless Grinding Operations. *IEEE Conference on Control* : 977–982.
[148] Li B, Zhang S, Fang Y, Wang J, Lu S (2019) Effects Of Cutting Parameters On Surface Quality In Hard Milling. *Materials and Manufacturing Processes* 34 (16):1803–1815.
[149] Li J, Lu J, Chen C, Ma J, Liao X (2021) Tool Wear State Prediction Based On Feature-Based Transfer Learning. *International Journal of Advanced Manufacturing Technology* 113(11-12):3283–3301.
[150] Li W, Li DY (2006) Influence Of Surface Morphology On Corrosion And Electronic Behavior. *Acta Materialia* 54(2):445–452.
[151] Li X, Rong Y (2011) Framework Of Grinding Process Modeling And Simulation Based On Microscopic Interaction Analysis. *Robotics and Computer-Integrated Manufacturing* 27(2):471–478.
[152] Liang SY, Su J-C (2007) Residual Stress Modeling in Orthogonal Machining. *CIRP Annals* 56(1):65–68.
[153] Liang X, Liu Z, Wang B (2019) State-Of-The-Art Of Surface Integrity Induced By Tool Wear Effects In Machining Process Of Titanium And Nickel Alloys: A Review. *Measurement* 132:150–181.
[154] Liang YC, Wang S, Li WD, Lu X (2019) Data-Driven Anomaly Diagnosis for Machining Processes. *Engineering* 5(4):646–652.
[155] Liao Z, La Monaca A, Murray J, Speidel A, Ushmaev D, Clare A, Axinte D, M'Saoubi R (2021) Surface Integrity In Metal Machining - Part I: Fundamentals Of Surface Characteristics And Formation Mechanisms. *International Journal of Machine Tools and Manufacture* 162:103687.
[156] Liao Z, Polyakov M, Diaz OG, Axinte D, Mohanty G, Maeder X, Michler J, Hardy M (2019) Grain Refinement Mechanism Of Nickel-Based Superalloy By Severe Plastic Deformation - Mechanical Machining Case. *Acta Materialia* 180:2–14.
[157] Liu Q, Chen X, Gindy N (2005) Fuzzy Pattern Recognition Of AE Signals For Grinding Burn. *International Journal of Machine Tools and Manufacture* 45 (7):811–818.
[158] Liu R, Salahshoor M, Melkote SN, Marusich T (2014) The Prediction of Machined Surface Hardness Using a New Physics-based Material Model. *Procedia CIRP* 13:249–256.
[159] Löhe D, Lang K-H, Vöhringer O (2002) Residual Stress And Fatigue Behavior. *Handbook of Residual Stress and Deformation of Steel* : 27–53.
[160] Lucca DA, Brinksmeier E, Goch G (1998) Progress in Assessing Surface and Subsurface Integrity. *CIRP Annals* 47(2):669–693.
[161] M'Saoubi R, Outeiro JC, Changeux B, Lebrun JL, Morão Dias A (1999) Residual Stress Analysis In Orthogonal Machining Of Standard And Resulfurized AISI 316L Steels. *Journal of Materials Processing Technology* 96(1-3):225–233.
[162] Mahata S, Shakya P, Babu NR, Prakasam PK (2020) In-Process Characterization Of Surface Finish In Cylindrical Grinding Process Using Vibration And Power Signals. *Procedia CIRP* 88:335–340.
[163] Malakizadi A, Bertolini R, Ducobu F, Kilic Z, Magnanini MC, Shokrani A (2022) Recent Advances In Modelling And Simulation Of Surface Integrity In Machining – A Review. *Procedia CIRP* 115:232–240.

Please cite this article as: V. Schulze et al., Surface conditioning in cutting and abrasive processes, CIRP Annals - Manufacturing Technology (2024), https://doi.org/10.1016/j.cirp.2024.05.004

[164] Malkin S, Guo C (2007) Thermal Analysis of Grinding. *CIRP Annals* 56(2): 760–782.
[165] Malkin S, Lenz E (1978) Burning Limit For Surface And Cylindrical Grinding Of Steels. *CIRP Annals* 27(1):233–236.
[166] Matsumoto Y, Hashimoto F, Lahoti G (1999) Surface Integrity Generated by Precision Hard Turning. *CIRP Annals* 48(1):59–62.
[167] Maurer G, Neff H, Scholtes B, Macherauch E (1988) Texture and Lattice Deformation Pole Figures of Machined Surfaces. *Textures and Microstructures* 8:685607.
[168] Mayer P, Kirsch B, Müller R, Becker S, Ev Harbou, Aurich JC (2016) Influence of Cutting Edge Geometry on Deformation Induced Hardening when Cryogenic Turning of Metastable Austenitic Stainless Steel AISI 347. *Procedia CIRP* 45:59–62.
[169] Mayer P, Skorupski R, Smaga M, Eifler D, Aurich JC (2014) Deformation Induced Surface Hardening when Turning Metastable Austenitic Steel AISI 347 with Different Cryogenic Cooling Strategies. *Procedia CIRP* 14:101–106.
[170] Melkote S, Liang S, Özel T, Jawahir IS, Stephenson DA, Wang B (2022) 100th Anniversary Issue of the Manufacturing Engineering Division Paper A Review of Advances in Modeling of Conventional Machining Processes: From Merchant to the Present. *Journal of Manufacturing Science and Engineering* 144(11).
[171] MENG Q, Guo B, Zhao Q, Li HN, JACKSON MJ, LINKE BS, Luo X (2022) Modelling Of Grinding Mechanics: A Review. *Chinese Journal of Aeronautics* .
[172] Merchant ME (1944) Basic Mechanics of the Metal-Cutting Process. *Journal of Applied Mechanics* 11(3):A168–A175.
[173] Meurer M, Tekkaya B, Augspurger T, Pullen T, Schraknepper D, Bergs T, Münstermann S (2020) Cutting Force Based Surface Integrity Soft-Sensor When Hard Machining AISI 4140. *tm - Technisches Messen* 87(11):683–693.
[174] Mirifar S, Kadivar M, Azarhoushang B (2020) First Steps through Intelligent Grinding Using Machine Learning via Integrated Acoustic Emission Sensors. *Journal of Manufacturing and Materials Processing* 4(2):35.
[175] Möhring H-C, Eschelbacher S, Georgi P (2021) Machine Learning Approaches For Real-Time Monitoring And Evaluation Of Surface Roughness Using A Sensory Milling Tool. *Procedia CIRP* 102:264–269.
[176] Mondelin A, Valiorgue F, Rech J, Coret M (2021) 3D Hybrid Numerical Model of Residual Stresses: Numerical—Sensitivity to Cutting Parameters When Turning 15-5PH Stainless Steel. *Journal of Manufacturing and Materials Processing* 5(3):70.
[177] M'Saoubi R, Larsson T, Outeiro J, Guo Y, Suslov S, Saldana C, Chandrasekar S (2012) Surface Integrity Analysis Of Machined Inconel 718 Over Multiple Length Scales. *CIRP Annals* 61(1):99–102.
[178] Nagaraj A, Min S (2022) Effect Of Crystallography On Residual Stresses During Ultra-Precision Machining Of Sapphire. *CIRP Annals* 71(1):101–104.
[179] Nasir V, Sassani F (2021) A Review On Deep Learning In Machining And Tool Monitoring: Methods, Opportunities, And Challenges. *The International Journal, Advanced Manufacturing Technology* 115(9-10):2683–2709.
[180] Neslušan M, Čížek J, Kolařík K, Minárik P, Čilliková M, Melikhova O (2017) Monitoring Of Grinding Burn Via Barkhausen Noise Emission In Case-Hardened Steel In Large-Bearing Production. *Journal of Materials Processing Technology* 240:104–117.
[181] Neslušan M, Mičietová A, Hadzima B, Mičieta B, Kejzlar P, Čapek J, Uríček J, Pastorek F (2019) Barkhausen Noise Emission in Hard-Milled Surfaces. *Materials* 12 (4):660.
[182] Neslušan M, Uríček J, Mičietová A, Minárik P, Píška M, Čilliková M (2020) Decomposition Of Cutting Forces With Respect To Chip Segmentation And White Layer Thickness When Hard Turning 100Cr6. *Journal of Manufacturing Processes* 50:475–484.
[183] Neyra Astudillo MR, Núñez NM, López Pumarega MI, Ferrari G, Ruzzante J, Gómez M (2022) Study Of Martensite Induced By Deformation With Magnetic Barkhausen Noise Technique. *Journal of Magnetism and Magnetic Materials* 556:169454.
[184] Nguyen V, Fernandez-Zelaia P, Melkote SN (2017) PVDF Sensor Based Characterization Of Chip Segmentation In Cutting Of Ti-6Al-4V Alloy. *CIRP Annals* 66 (1):73–76.
[185] Nguyen V-H, Le T-T, Truong H-S, Le MV, Ngo V-L, Nguyen AT, Nguyen HQ (2021) Applying Bayesian Optimization for Machine Learning Models in Predicting the Surface Roughness in Single-Point Diamond Turning Polycarbonate. *Mathematical Problems in Engineering* 2021:1–16.
[186] Niesłony P, Grzesik W, Laskowski P, Sienawski J (2014) Numerical and Experimental Analysis of Residual Stresses Generated in the Machining of Ti6Al4V Titanium Alloy. *Procedia CIRP* 13:78–83.
[187] Novovic D, Aspinwall DK, Dewes RC, Bowen P, Griffiths B (2016) The Effect Of Surface And Subsurface Condition On The Fatigue Life Of Ti−25V−15Cr−2Al−0.2C %wt Alloy. *CIRP Annals* 65(1):523–528.
[188] Novovic D, Dewes RC, Aspinwall DK, Voice W, Bowen P (2004) The Effect Of Machined Topography And Integrity On Fatigue Life. *International Journal of Machine Tools and Manufacture* 44(2-3):125–134.
[189] Nowag L, Solter J, Walter A, Brinksmeier E (2006) Effect Of Machining Parameters And Clamping Technique On Residual Stresses And Distortion Of Bearing Rings. *Mat.-wiss. u. Werkstofftech.* 37(1):45–51.
[190] Outeiro JC, Dias AM, Lebrun JL, Astakhov VP (2002) Machining Residual Stresses In Aisi 316l Steel And Their Correlation With The Cutting Parameters. *Machining Science and Technology* 6(2):251–270.
[191] Outeiro JC, Umbrello D, M'Saoubi R (2006) Experimental And Numerical Modelling Of The Residual Stresses Induced In Orthogonal Cutting Of AISI 316L Steel. *International Journal of Machine Tools and Manufacture* 46 (14):1786–1794.
[192] Outeiro JC, Umbrello D, M'Saoubi R, Jawahir IS (2015) Evaluation of Present Numerical Models for Predicting Metal Cutting Performance And Residual Stresses. *Machining Science and Technology* 19(2):183–216.
[193] Panchal G, Ganatra A, Shah P, Panchal D (2011) Determination of Over-Learning and Over-Fitting Problem in Back Propagation Neurl Network. *International Journal on Soft Computing* 2(2):40–51.
[194] Perevertov O, Neslušan M, Stupakov A (2017) Detection Of Milled 100Cr6 Steel Surface By Eddy Current And Incremental Permeance Methods. *Independent Nondestructive Testing and Evaluation International* 87:15–23.
[195] Pimenov DY, Bustillo A, Mikolajczyk T (2018) Artificial Intelligence For Automatic Prediction Of Required Surface Roughness By Monitoring Wear On Face Mill Teeth. *Journal of Intelligent Manufacturing* 29(5):1045–1061.
[196] Plogmeyer M, González G, Schulze V, Bräuer G (2020) Development Of Thin-Film Based Sensors For Temperature And Tool Wear Monitoring During Machining. *tm - Technisches Messen* 87(12):768–776.
[197] Prevéy PS, Cammett JT (2004) The Influence Of Surface Enhancement By Low Plasticity Burnishing On The Corrosion Fatigue Performance Of AA7075-T6. *International Journal of Fatigue* 26(9):975–982.
[198] Psichogios DC, Ungar LH (1992) A Hybrid Neural Network-First Principles Approach To Process Modeling. *American Institute of Chemical Engineers Journal* 38(10):1499–1511.
[199] Pu Z, Outeiro JC, Batista AC, Dillon OW, Puleo DA, Jawahir IS (2012) Enhanced Surface Integrity Of AZ31B Mg Alloy By Cryogenic Machining Towards Improved Functional Performance Of Machined Components. *International Journal of Machine Tools and Manufacture* 56:17–27.
[200] Pu Z, Umbrello D, Dillon OW, Lu T, Puleo DA, Jawahir IS (2014) Finite Element Modeling Of Microstructural Changes In Dry And Cryogenic Machining Of AZ31B Magnesium Alloy. *Journal of Manufacturing Processes* 16(2):335–343.
[201] Rajesh AS, Prabhuswamy MS, Krishnasamy S (2022) Smart Manufacturing through Machine Learning: A Review, Perspective, and Future Directions to the Machining Industry. *Journal of Engineering* 2022:1–6.
[202] Ramesh A, Melkote SN (2008) Modeling Of White Layer Formation Under Thermally Dominant Conditions In Orthogonal Machining Of Hardened AISI 52100 Steel. *International Journal of Machine Tools and Manufacture* 48 (3-4):402–414.
[203] Rami A, Kallel A, Sghaier S, Youssef S, Hamdi H (2017) Residual Stresses Computation Induced By Turning Of AISI 4140 Steel Using 3D Simulation Based On A Mixed Approach. *International Journal of Advanced Manufacturing Technology* 91 (9-12):3833–3850.
[204] Rech J, Moisan A (2003) Surface Integrity In Finish Hard Turning Of Case-Hardened Steels. *International Journal of Machine Tools and Manufacture* 43(5):543–550.
[205] Reimer A, Luo X (2018) Prediction Of Residual Stress In Precision Milling Of AISI H13 Steel. *Procedia CIRP* 71:329–334.
[206] Rigney DA, Fu XY, Hammerberg JE, Holian BL, Falk ML (2003) Examples Of Structural Evolution During Sliding And Shear Of Ductile Materials. *Scripta Materialia* 49(10):977–983.
[207] Rinaldi S, Imbrogno S, Rotella G, Umbrello D, Filice L (2019) Physics Based Modeling Of Machining Inconel 718 To Predict Surface Integrity Modification. *Procedia CIRP* 82:350–355.
[208] Rotella G, Dillon OW, Umbrello D, Settineri L, Jawahir IS (2013) Finite Element Modeling Of Microstructural Changes In Turning Of AA7075-T651 Alloy. *Journal of Manufacturing Processes* 15(1):87–95.
[209] Sadeghifar M, Sedaghati R, Jomaa W, Songmene V (2018) A Comprehensive Review Of Finite Element Modeling Of Orthogonal Machining Process: Chip Formation And Surface Integrity Predictions. *International Journal of Advanced Manufacturing Technology* 96(9-12):3747–3791.
[210] Safarzadeh H, Leonesio M, Bianchi G, Monno M (2021) Roundness Prediction In Centreless Grinding Using Physics-Enhanced Machine Learning Techniques. *International Journal of Advanced Manufacturing Technology* 112 (3-4):1051–1063.
[211] Saini S, Ahuja IS, Sharma VS (2012) Residual Stresses, Surface Roughness, and Tool Wear in Hard Turning: A Comprehensive Review. *Materials and Manufacturing Processes* 27(6):583–598.
[212] Sales WF, Schoop J, da Silva LR, Machado ÁR, Jawahir IS (2020) A Review Of Surface Integrity In Machining Of Hardened Steels. *Journal of Manufacturing Processes* 58:136–162.
[213] Salvatore F, Halila F, Mabrouki T, Hamdi H (2012) Numerical And Experimental Study Of Residual Stress Induced By Machining Process. *International Journal of Surface Science and Engineering* 6(1/2):136.
[214] Sasahara H (2005) The Effect On Fatigue Life Of Residual Stress And Surface Hardness Resulting From Different Cutting Conditions Of 0.45%C Steel. *International Journal of Machine Tools and Manufacture* 45(2):131–136.
[215] Sasaki K, Burstein GT (1996) The Generation Of Surface Roughness During Slurry Erosion-Corrosion And Its Effect On The Pitting Potential. *Corrosion Science* 38 (12):2111–2120.
[216] Sauter E, Sarikaya E, Winter M, Wegener K (2021) In-Process Detection Of Grinding Burn Using Machine Learning. *International Journal of Advanced Manufacturing Technology* 115(7-8):2281–2297.
[217] Scherge M (2018) The Running-in of Lubricated Metal-Metal Contacts—A Review on Ultra-Low Wear Systems. *Lubricants* 6(2):54.
[218] Scherge M, Shakhvorostov D, Pöhlmann K (2003) Fundamental Wear Mechanism Of Metals. *Wear* 255(1-6):395–400.
[219] Schmidt R, Brause L, Strodick S, Walther F, Biermann D, Zabel A (2022) Measurement And Analysis Of The Thermal Load In The Bore Subsurface Zone During Bta Deep Hole Drilling. *Procedia CIRP* 107:375–380.

Please cite this article as: V. Schulze et al., Surface conditioning in cutting and abrasive processes, CIRP Annals - Manufacturing Technology (2024), https://doi.org/10.1016/j.cirp.2024.05.004

[220] Schmidt R, Strodick S, Walther F, Biermann D, Zabel A (2020) Influence Of The Process Parameters And Forces On The Bore Sub-Surface Zone In BTA Deep-Hole Drilling Of AISI 4140 and AISI 304L. *Procedia CIRP* 87:41–46.
[221] Schölkopf B, Herbrich R, Smola AJ (2001) A Generalized Representer Theorem. in Helmbold D, Williamson B, (Eds.) *Computational learning theory: Proceedings*, Springer, , 416–426.
[222] Scholtes B (1991) *Eigenspannungen in Mechanisch Randschichtverformten Werkstoffzuständen: Ursachen, Ermittlung und Bewertung. DGM-Informationsges*, Oberursel.
[223] Scholtes B, Macherauch E (1986) Auswirkungen mechanischer Randschichtverformungen auf das Festigkeitsverhalten metallischer Werkstoffe. *Zeitschrift für Metallkunde* : 322–337. 77-5.
[224] Schorr S, Möller M, Heib J, Bähre D (2020) Quality Prediction of Drilled and Reamed Bores Based on Torque Measurements and the Machine Learning Method of Random Forest. *Procedia Manufacturing* 48:894–901.
[225] Schulz H, Behnke S (2012) Deep Learning. *Künstl Intell* 26(4):357–363.
[226] Schulze V (2006) *Modern Mechanical Surface Treatment: States, Stability, Effects*, 1st ed. Wiley-VCHWeinheim.
[227] Schulze V, Hoffmeister J, Klemenz M (2011) Correlation of Mechanical Surface Treatments, induced Surface States and Fatigue Performance of Steel Components. *Procedia Engineering* 19:324–330.
[228] Schulze V, Zanger F, Stampfer B, Seewig J, Uebel J, Zabel A, Wolter B, Böttger D (2020) Surface Conditioning In Machining Processes. *tm - Technisches Messen* 87 (11):661–673.
[229] Schwach DW, Guo Y (2006) A Fundamental Study On The Impact Of Surface Integrity By Hard Turning On Rolling Contact Fatigue. *International Journal of Fatigue* 28(12):1838–1844.
[230] Schwär D, González G, Segebade E, Zanger F, Heizmann M (2020) Evaluation Of The Acoustic Emission Caused By The Chip Segmentation Frequency During Machining Of Titanium Alloy. *tm - Technisches Messen* 87(11):714–720.
[231] Schwenk M (2012) *Numerische Modellierung der Induktiven Ein- und Zweifrequenzrandschichthärtung*, KIT Scientific PublishingKarlsruhe.
[232] Seewig J, Eifler M, Schneider F, Kirsch B, Aurich JC (2016) A Model-Based Approach For The Calibration And Traceability Of The Angle Resolved Scattering Light Sensor. *Surface Topography: Metrology and Properties* 4(2):24010.
[233] Serin G, Sener B, Ozbayoglu AM, Unver HO (2020) Review Of Tool Condition Monitoring In Machining And Opportunities For Deep Learning. *International Journal of Advanced Manufacturing Technology* 109(3-4):953–974.
[234] Setti D, Arrabiyeh PA, Kirsch B, Heintz M, Aurich JC (2020) Analytical And Experimental Investigations On The Mechanisms Of Surface Generation In Micro Grinding. *International Journal of Machine Tools and Manufacture* 149:103489.
[235] Shahin M, Chen FF, Bouzary H, Krishnaiyer K (2020) Integration Of Lean Practices And Industry 4.0 Technologies: Smart Manufacturing For Next-Generation Enterprises. *International Journal of Advanced Manufacturing Technology* 107(5-6):2927–2936.
[236] Shahryari A, Kamal W, Omanovic S (2008) The Effect Of Surface Roughness On The Efficiency Of The Cyclic Potentiodynamic Passivation (CPP) Method In The Improvement Of General And Pitting Corrosion Resistance Of 316LVM Stainless Steel. *Materials Letters* 62(23):3906–3909.
[237] Shao C, Paynabar K, Kim TH, Jin J, Hu SJ, Spicer JP, Wang H, Abell JA (2013) Feature Selection For Manufacturing Process Monitoring Using Cross-Validation. *Journal of Manufacturing Systems* 32(4):550–555.
[238] Shao T, Krishnamurty S (2008) A Clustering-Based Surrogate Model Updating Approach to Simulation-Based Engineering Design. *Journal of Mechanical Design* 130(4).
[239] Sharman A, Hughes JI, Ridgway K (2006) An Analysis Of The Residual Stresses Generated In Inconel 718™ When Turning. *Journal of Materials Processing Technology* 173(3):359–367.
[240] Shen N, Ding H, Pu Z, Jawahir IS, Jia T (2017) Enhanced Surface Integrity From Cryogenic Machining of AZ31B Mg Alloy: A Physics-Based Analysis With Microstructure Prediction. *Journal of Manufacturing Science and Engineering* 139 (6):61012.
[241] Shi B, Abboud E, Attia MH, Thomson V (2022) Effect of Chip Segmentation on Machining-Induced Residual Stresses during Turning of Ti6Al4V. *Procedia CIRP* 108:424–429.
[242] SME. *The American National Standard for Surface Integrity(ANSI B211.1-1986)*, Dearborn, USA.
[243] Smith KN, Topper T, Watson P (1970) A Stress–Strain Function For The Fatigue Of Metals (Stress-Strain Function For Metal Fatigue Including Mean Stress Effect). *Materials* 5:767–778.
[244] Smith RJ, Hirsch M, Patel R, Li W, Clare AT, Sharples SD (2016) Spatially Resolved Acoustic Spectroscopy For Selective Laser Melting. *Journal of Materials Processing Technology* 236:93–102.
[245] Smith S, Melkote SN, Lara-Curzio S, Watkins TR, Allard L, Riester L (2007) Effect Of Surface Integrity Of Hard Turned AISI 52100 Steel On Fatigue Performance. *Materials Science and Engineering: A* 459(1-2):337–346.
[246] Stampfer B, Bachmann J, Gauder D, Böttger D, Gerstenmeyer M, Lanza G, Wolter B, Schulze V (2022) Modeling Of Surface Hardening And Roughness Induced By Turning AISI 4140 QT Under Different Machining Conditions. *Procedia CIRP* 108:293–298.
[247] Stampfer B, Böttger D, Gauder D, Zanger F, Häfner B, Straß B, Wolter B, Lanza G, Schulze V (2020) Experimental Identification Of A Surface Integrity Model For Turning Of AISI4140. *Procedia CIRP* 87(5):83–88.
[248] Stampfer B, González G, Gerstenmeyer M, Schulze V (2021) The Present State of Surface Conditioning in Cutting and Grinding. *Journal of Manufacturing and Materials Processing* .
[249] Stampfer B, González G, Segebade E, Gerstenmeyer M, Schulze V (2021) Material Parameter Optimization For Orthogonal Cutting Simulations Of AISI4140 At Various Tempering Conditions. *Procedia CIRP* 102(10):198–203.
[250] Strodick S, Berteld K, Schmidt R, Biermann D, Zabel A, Walther F (2020) Influence Of Cutting Parameters On The Formation Of White Etching Layers In BTA Deep Hole Drilling. *tm - Technisches Messen* 87(11):674–682.
[251] Stupakov A, Neslušan M, Perevertov O (2016) Detection Of A Milling-Induced Surface Damage By The Magnetic Barkhausen Noise. *Journal of Magnetism and Magnetic Materials* 410:198–209.
[252] Tampu C, Chirita B, Cristea I, Zichil V, Schnakovszky C, Herghelegiu E, Carausu C (2020) Influence Of Cutting Parameters On Surface Hardness In Milling Of AL6061T6. *IOP Conference Series: Materials Science and Engineering* 916(1): 12118.
[253] Tanaka K (2018) The cosα Method for X-ray Residual Stress Measurement Using Two-Dimensional Detector. *Mechanical Engineering Reviews* . advpub.
[254] Távora CG, Aguiar PR, Castro BA, Alexandre FA, Andreoli AL, Bianchi EC (2021) Hinkley Criterion Applied To Detection And Location Of Burn In Grinding Process. *International Journal of Advanced Manufacturing Technology* 113(11):3177–3188.
[255] Tekkaya B, Meurer M, Dölz M, Könemann M, Münstermann S, Bergs T (2023) Modeling Of Microstructural Workpiece Rim Zone Modifications During Hard Machining. *Journal of Materials Processing Technology* 311:117815.
[256] Tekkaya B, Meurer M, Münstermann S (2020) Modelling of Grain Size Evolution with Different Approaches via FEM When Hard Machining of AISI 4140. *Metals* 10(10):1296.
[257] Thakur A, Gangopadhyay S (2016) State-Of-The-Art In Surface Integrity In Machining Of Nickel-Based Super Alloys. *International Journal of Machine Tools and Manufacture* 100:25–54.
[258] Tönshoff H, Jung M, Männel S, Rietz W (2000) Using Acoustic Emission Signals For Monitoring Of Production Processes. *Ultrasonics* 37(10):681–686.
[259] Tönshoff HK, Arendt C, Amor RB (2000) Cutting of Hardened Steel. *CIRP Annals* 49(2):547–566.
[260] Tönshoff HK, Karpuschewski B, Wobker H-G (1995) Quality Control of Surface Integrity with Micromagnetic Techniques. *Production Engineering, Annals of the German Academic Society for Production Engineering* 2:203–206.
[261] Tönshoff HK, Peters J, Inasaki I, Paul T (1992) Modelling and Simulation of Grinding Processes. *CIRP Annals* 41(2):677–688.
[262] Tosello G, Bissacco G, Cao J, Axinte D (2023) Modeling And Simulation Of Surface Generation In Manufacturing. *CIRP Annals* 72(2):753–779.
[263] Uebel J, Ankener W, Basten S, Smaga M, Kirsch B, Seewig J, Beck T, Aurich JC (2020) In-Process And Ex-Situ Measurement Techniques For The Characterization Of Surface Conditions During Cryogenic Hard Turning Of AISI 52100. *tm - Technisches Messen* 87(11):694–703.
[264] Uebel J, Ströer F, Basten S, Ankener W, Hotz H, Heberger L, Stelzer G, Kirsch B, Smaga M, Seewig J, Aurich JC, Beck T (2019) Approach For The Observation Of Surface Conditions In-Process By Soft Sensors During Cryogenic Hard Turning. *Procedia CIRP* 81:1260–1265.
[265] Uhlmann E, Holznagel T, Schehl P, Bode Y (2021) Machine Learning of Surface Layer Property Prediction for Milling Operations. *Journal of Manufacturing and Materials Processing* 5(4):104.
[266] Ulas M, Aydur O, Gurgenc T, Ozel C (2020) Surface Roughness Prediction Of Machined Aluminum Alloy With Wire Electrical Discharge Machining By Different Machine Learning Algorithms. *Journal of Materials Research and Technology* 9 (6):12512–12524.
[267] Ullrich K, Elling M, Gutzeit K, Dix M, Weigold M, Aurich JC, Wertheim R, Jawahir IS, Ghadbeigi H (2024) AI-Based Multi-Objective Optimisation Of Total Machining Performance. *CIRP Journal of Manufacturing Science and Technology* 50: 40–54.
[268] Ulutan D, Ozel T (2011) Machining Induced Surface Integrity In Titanium And Nickel Alloys: A Review. *International Journal of Machine Tools and Manufacture* 51(3):250–280.
[269] Umbrello D (2013) Analysis Of The White Layers Formed During Machining Of Hardened AISI 52100 Steel Under Dry And Cryogenic Cooling Conditions. *International Journal of Advanced Manufacturing Technology* 64(5-8):633–642.
[270] Umbrello D (2014) The Effects of Cutting Conditions on Surface Integrity in Machining Waspaloy. *Key Engineering Materials* 611-612:1243–1249.
[271] Umbrello D, Ambrogio G, Filice L, Shivpuri R (2008) A Hybrid Finite Element Method–Artificial Neural Network Approach For Predicting Residual Stresses And The Optimal Cutting Conditions During Hard Turning Of AISI 52100 Bearing Steel. *Materials & Design* 29(4):873–883.
[272] Umbrello D, Filice L (2009) Improving Surface Integrity In Orthogonal Machining Of Hardened AISI 52100 Steel By Modeling White And Dark Layers Formation. *CIRP Annals* 58(1):73–76.
[273] Umbrello D, Hua J, Shivpuri R (2004) Hardness-Based Flow Stress And Fracture Models For Numerical Simulation Of Hard Machining AISI 52100 Bearing Steel. *Materials Science and Engineering: A* 374(1-2):90–100.
[274] Umbrello D, Jawahir IS (2009) Numerical Modeling Of The Influence Of Process Parameters And Workpiece Hardness On White Layer Formation In AISI 52100 Steel. *International Journal of Advanced Manufacturing Technology* 44(9-10):955–968.
[275] Umbrello D, Jayal AD, Caruso S, Dillon OW, Jawahir IS (2010) Modeling Of White And Dark Layer Formation In Hard Machining Of AISI 52100 Bearing Steel. *Machining Science and Technology* 14(1):128–147.
[276] Umbrello D, Outeiro JC, M'Saoubi R, Jayal AD, Jawahir IS (2010) A numerical Model Incorporating The Microstructure Alteration For Predicting Residual Stresses In Hard Machining Of AISI 52100 Steel. *CIRP Annals* 59(1):113–116.

Please cite this article as: V. Schulze et al., Surface conditioning in cutting and abrasive processes, CIRP Annals - Manufacturing Technology (2024), https://doi.org/10.1016/j.cirp.2024.05.004

[277] Umbrello D, Pu Z, Caruso S, Outeiro JC, Jayal AD, Dillon OW, Jawahir IS (2011) The Effects of Cryogenic Cooling on Surface Integrity in Hard Machining. *Procedia Engineering* 19:371–376.
[278] Valiorgue F, Rech J, Hamdi H, Gilles P, Bergheau JM (2007) A New Approach For The Modelling Of Residual Stresses Induced By Turning Of 316L. *Journal of Materials Processing Technology* 191(1-3):270–273.
[279] van Luttervelt CA, Childs T, Jawahir IS, Klocke F, Venuvinod PK, Altintas Y, Armarego E, Dornfeld D, Grabec I, Leopold J, Lindstrom B, Lucca D, Obikawa T, Shirakashi Sato H (1998) Present Situation and Future Trends in Modelling of Machining Operations Progress Report of the CIRP Working Group 'Modelling of Machining Operations. *CIRP Annals* 47(2):587–626.
[280] Vasanth XA, Paul PS, Varadarajan AS (2020) A Neural Network Model To Predict Surface Roughness During Turning Of Hardened SS410 Steel. *International Journal of System Assurance Engineering and Management* 11(3):704–715.
[281] Vovk A, Sölter J, Karpuschewski B (2020) Finite Element Simulations Of The Material Loads And Residual Stresses In Milling Utilizing The CEL Method. *Procedia CIRP* 87(3):539–544.
[282] Vovk A, Sölter J, Karpuschewski B (2021) Numerical Investigation Of The Influence Of Multiple Loads On Material Modifications During Hard Milling. *Procedia CIRP* 102(1):500–505.
[283] Walter R, Kannan MB (2011) Influence Of Surface Roughness On The Corrosion Behaviour Of Magnesium Alloy. *Materials & Design* 32(4):2350–2354.
[284] Wang C, Bao Z, Zhang P, Ming W, Chen M (2019) Tool Wear Evaluation Under Minimum Quantity Lubrication By Clustering Energy Of Acoustic Emission Burst Signals. *Measurement* 138:256–265.
[285] Wang J, Zhang D, Wu B, Luo M (2017) Numerical and Empirical Modelling of Machining-induced Residual Stresses in Ball end Milling of Inconel 718. *Procedia CIRP* 58:7–12.
[286] Wang X, Eisseler R, Moehring H-C (2020) Prediction And Optimization Of Machining Results And Parameters In Drilling By Using Bayesian Networks. *Production Engineering* 14(3):373–383.
[287] Wang Z, Willett P, DeAguiar PR, Webster J (2001) Neural Network Detection Of Grinding Burn From Acoustic Emission. *International Journal of Machine Tools and Manufacture* 41(2):283–309.
[288] Warnecke G, Zitt U (1998) Kinematic Simulation for Analyzing and Predicting High-Performance Grinding Processes. *CIRP Annals* 47(1):265–270.
[289] Wegert R, Guski V, Möhring H-C, Schmauder S (2020) Temperature Monitoring In The Subsurface During Single Lip Deep Hole Drilling. *tm - Technisches Messen* 87(12):757–767.
[290] Weichert D, Link P, Stoll A, Rüping S, Ihlenfeldt S, Wrobel S (2019) A Review Of Machine Learning For The Optimization Of Production Processes. *International Journal of Advanced Manufacturing Technology* 104(5-8):1889–1902.
[291] Wolter B, Gabi Y, Conrad C (2019) Nondestructive Testing with 3MA—An Overview of Principles and Applications. *Applied Sciences* 9(6):1068.
[292] Xie N, Zhou J, Zheng B (2018) An Energy-Based Modeling And Prediction Approach For Surface Roughness In Turning. *International Journal of Advanced Manufacturing Technology* 96(5-8):2293–2306.
[293] Xu D, Edwards TE, Liao Z, Maeder X, Ramachandramoorthy R, Jain M, Michler J, Axinte D (2021) Revealing Nanoscale Deformation Mechanisms Caused By Shear-Based Material Removal On Individual Grains Of A Ni-Based Superalloy. *Acta Materialia* 212:116929.
[294] Xu X, Outeiro J, Zhang J, Xu B, Zhao W, Astakhov V (2021) Machining Simulation Of Ti6Al4V Using Coupled Eulerian-Lagrangian Approach And A Constitutive Model Considering The State Of Stress. *Simulation Modelling Practice and Theory* 110:102312.
[295] Xu X, Zhang J, Outeiro J, Xu B, Zhao W (2020) Multiscale Simulation Of Grain Refinement Induced By Dynamic Recrystallization Of Ti6Al4V Alloy During High Speed Machining. *Journal of Materials Processing Technology* 286:116834.
[296] Yan J, Asami T, Kuriyagawa T (2008) Nondestructive Measurement Of Machining-Induced Amorphous Layers In Single-Crystal Silicon By Laser Micro-Raman Spectroscopy. *Precision Engineering* 32(3):186–195.
[297] Yan J, Li L (2013) Multi-Objective Optimization Of Milling Parameters – The Trade-Offs Between Energy, Production Rate And Cutting Quality. *Journal of Cleaner Production* 52:462–471.
[298] Yan J, Takahashi H, Tamaki J, Gai X, Harada H, Patten J (2005) Nanoindentation Tests On Diamond-Machined Silicon Wafers. *Applied Physics Letters* 86 (18):181913.
[299] Yang D, Liu Z, Ren X, Zhuang P (2016) Hybrid Modeling With Finite Element And Statistical Methods For Residual Stress Prediction In Peripheral Milling Of Titanium Alloy Ti-6Al-4V. *International Journal of Mechanical Sciences* 108-109:29–38.
[300] Yang Z, Eddy D, Krishnamurty S, Grosse I, Denno P, Lu Y, Witherell P (2017) Investigating Grey-Box Modeling for Predictive Analytics in Smart Manufacturing. *Volume 2B: 43rd Design Automation Conference*, American Society of Mechanical Engineers, .
[301] Yang Z, Wu H, Yu Z, Huang Y (2014) A Non-Destructive Surface Burn Detection Method For Ferrous Metals Based On Acoustic Emission And Ensemble Empirical Mode Decomposition: From Laser Simulation To Grinding Process. *Surface Topography: Metrology and Properties* 25(3):35602.
[302] Yin Q, Liu Z, Wang B, Song Q, Cai Y (2020) Recent Progress Of Machinability And Surface Integrity For Mechanical Machining Inconel 718: A Review. *International Journal of Advanced Manufacturing Technology* 109(1-2):215–245.
[303] Zanger F, Kacaras A, Neuenfeldt P, Schulze V (2019) Optimization Of The Stream Finishing Process For Mechanical Surface Treatment By Numerical And Experimental Process Analysis. *CIRP Annals* 68(1):373–376.
[304] Zhang L, Hashimoto T, Yan J (2021) Machinability Exploration For High-Entropy Alloy FeCrCoMnNi By Ultrasonic Vibration-Assisted Diamond Turning. *CIRP Annals* 70(1):37–40.
[305] Zhang Z, Wang Z, Wang W, Jiang R, Xiong Y (2020) Investigation On Surface Quality Of High-Speed Cutting Titanium Alloy Ti6Al4V Based On Split-Hopkinson Pressure Bar. *Proceedings of the Institution of Mechanical Engineers, Part B: Journal of Engineering Manufacture* 234(10):1293–1301.
[306] Zhao Y-Z, Guo K, Sivalingam V, Li J-F, Sun Q-D, Zhu Z-J, Sun J (2021) Surface Integrity Evolution Of Machined NiTi Shape Memory Alloys After Turning Process. *Advances in Manufacturing* 9(3):446–456.
[307] Zhou T, He L, Wu J, Du F, Zou Z (2019) Prediction of Surface Roughness of 304 Stainless Steel and Multi-Objective Optimization of Cutting Parameters Based on GA-GBRT. *Applied Sciences* 9(18):3684.
[308] Zhou X, Xi F (2002) Modeling And Predicting Surface Roughness Of The Grinding Process. *International Journal of Machine Tools and Manufacture* 42(8):969–977.
[309] Zielinski T, Vovk A, Riemer O, Karpuschewski B (2021) An Investigation on Internal Material Loads and Modifications in Precision Turning of Steel 42CrMo4. *Micromachines* 12(5).
[310] Zuo Y, Wang H, Xiong J (2002) The Aspect Ratio Of Surface Grooves And Metastable Pitting Of Stainless Steel. *Corrosion Science* 44(1):25–35.

Please cite this article as: V. Schulze et al., Surface conditioning in cutting and abrasive processes, CIRP Annals - Manufacturing Technology (2024), https://doi.org/10.1016/j.cirp.2024.05.004